Available online at www.sciencedirect.com
ScienceDirect
Developmental Biology 307 (2007) 62–78
DEVELOPMENTAL BIOLOGY
www.elsevier.com/locate/ydbio

Dystroglycan regulates structure, proliferation and differentiation of neuroepithelial cells in the developing vertebrate CNS

Jörn E. Schröder [a,1,2], Marion R. Tegeler [a,2], Uli Groβhans [a], Elmar Porten [a], Martina Blank [a,3], Jun Lee [a], Chris Esapa [b], Derek J. Blake [b], Stephan Kröger [a,*]

[a] Department of Physiological Chemistry, University of Mainz, Duesbergweg 6, D-55099 Mainz, Germany
[b] Department of Pharmacology, University of Oxford, Mansfield Road, Oxford OX1 3QT, England, UK

Received for publication 19 February 2007; revised 8 April 2007; accepted 16 April 2007
Available online 24 April 2007

Abstract

In the developing CNS α- and β-dystroglycan are highly concentrated in the endfeet of radial neuroepithelial cells at the contact site to the basal lamina. We show that injection of anti-dystroglycan Fab fragments, knockdown of dystroglycan using RNAi, and overexpression of a dominant-negative dystroglycan protein by microelectroporation in neuroepithelial cells of the chick retina and optic tectum *in vivo* leads to the loss of their radial morphology, to hyperproliferation, to an increased number of postmitotic neurons, and to an altered distribution of several basally concentrated proteins. Moreover, these treatments also altered the oriented growth of axons from retinal ganglion cells and from tectal projection neurons. In contrast, expression of non-cleavable dystroglycan protein in neuroepithelial cells reduced their proliferation and their differentiation to postmitotic neurons. These results demonstrate that dystroglycan plays a key role in maintaining neuroepithelial cell morphology, and that interfering with dystroglycan function influences proliferation and differentiation of neuroepithelial cells. These data also suggest that an impaired dystroglycan function in neuroepithelial cells might be responsible for some of the severe brain abnormalities observed in certain forms of congenital muscular dystrophy.

Keywords: Muscular dystrophy; Development; RNAi; Dystrophin-associated protein complex; Retina; Axonal growth; Stem cells

Introduction

The dystrophin-associated glycoprotein complex (DGC) is a large and heteromeric protein complex which is widely expressed in many tissues. The central protein of all DGCs is dystroglycan, a membrane-associated receptor expressed in many tissues, with a complex structure and biosynthesis (for review see Cohn, 2005; Barresi and Campbell, 2006). Dystroglycan is translated from a single gene transcript but cleavage of the precursor protein by an unknown protease during or shortly after translation generates two subunits, α-dystroglycan and β-dystroglycan (Ibraghimov-Beskrovnaya et al., 1992). The β-dystroglycan subunit is a 43 kDa transmembrane protein with a single membrane spanning region. In contrast, α-dystroglycan is a heavily glycosylated extracellular protein with a molecular mass varying between 120 and 180 kDa, depending on the degree of glycosylation. In skeletal muscle, β-dystroglycan binds intracellularly with its C-terminus to the β-spectrin/α-actinin-like peripheral membrane proteins dystrophin or utrophin (Huang et al., 2000). Dystrophin and utrophin interact via their N-termini with the subsarcolemmal actin filaments (Rybakova et al., 1996). On the extracellular side, β-dystroglycan interacts non-covalently with α-dystroglycan (Sciandra et al., 2001) and α-dystroglycan has the potential to bind to several extracellular proteins, including laminin-1 and -2, agrin, biglycan, perlecan, and neurexins (Sugiyama et al.,

* Corresponding author. Present address: Institute for Physiology, Ludwig-Maximilians-University Munich, Schillerstrasse 46, D-80336 Munich, Germany. Fax: +49 89 2180 75216.
E-mail address: stephan.kroeger@lrz.uni-muenchen.de (S. Kröger).
[1] Present address: Glaxo Smith Kline, Neurology&GI CEDD, Harlow, CM19 5AW, England, UK.
[2] Both authors contributed equally to this work.
[3] Present address: Department of Psychiatry and Behavioral Sciences, Stanford University School of Medicine, 1201 Welch Rd., Stanford, CA 94305-5485, USA.

0012-1606/$ - see front matter © 2007 Elsevier Inc. All rights reserved.
doi:10.1016/j.ydbio.2007.04.020

1994; Talts et al., 1999; Sugita et al., 2001). These various interactions enable the DGC to form a continuous molecular link between the subsarcolemmal actin cytoskeleton and the extracellular matrix. In skeletal muscle this link provides mechanical stability to the muscle fibers particularly during contraction and relaxation (Ervasti and Campbell, 1993). Another function of the DGC is to provide a scaffold to which proteins can bind and, thus, become localized to the muscle fiber subsarcolemmal compartment (see for example Rando, 2001; Spence et al., 2004; Judge et al., 2006). Disruption of the DGC in skeletal muscle therefore has many more consequences than just the loss of basal lamina attachment. Accordingly, mutations which interfere with the function of the DGC cause various forms of muscular dystrophy, often fatal diseases characterized primarily by a progressive weakening and loss of skeletal muscle tissue (Dalkilic and Kunkel, 2003).

Dystroglycan and other DGC proteins are also expressed in non-muscle tissues, including the central nervous system (Blake and Kröger, 2000; Cohn, 2005). Accordingly, muscular dystrophies are frequently associated with a wide spectrum of CNS defects (Anderson et al., 2002). The CNS deficits are particularly severe in recently identified dystroglycanopathies, which include three forms of congenital muscular dystrophies: Walker–Warburg Syndrome, Muscle–Eye–Brain disease and Fukuyama-Congenital Muscular Dystrophy (Muntoni et al., 2004). These diseases are caused by mutations in glycosyltransferases that have α-dystroglycan as one of their main substrates in the CNS (Michele et al., 2002; Moore et al., 2002; Martin-Rendon and Blake, 2003). The CNS abnormalities in patients or animals with mutations in any of the glycosyltransferases are severe and include mental retardation, polymicrogyria, defects in neuronal migration, disorganization of CNS lamination, various degrees of cortical dysplasia, and extrusion of neuronal and glial tissue into the subarachinoidal space through breaches of the pia basal lamina (the glia limitans separating the brain parenchyma from the subarachinoid space; Yoshida et al., 2001; Beltran-Valero et al., 2002; Michele et al., 2002; Muntoni et al., 2004). Ocular abnormalities including a loss of the normal histoarchitecture and layering, hyperproliferation, altered neuronal migration and differentiation and retinal detachment are also frequently observed (Longman et al., 2003; Takeda et al., 2003; Beltran-Valero de Bernabe et al., 2004; Lee et al., 2005). Thus, a stable association of α-dystroglycan with the extracellular matrix via its carbohydrate side chains appears to be necessary for normal CNS development. However, the specific functions of dystroglycan, particularly in the early developing CNS, and the mechanism, that lead to the severe brain abnormalities in congenital muscular dystrophies are unknown.

Neuroepithelial cells are the principal cells of the neural plate and neural tube and represent the precursor cells for neurons and glial cells in the developing CNS (for review see Kriegstein and Götz, 2003; Götz and Huttner, 2005). Neuroepithelial cells have a palisade-like morphology with their processes spanning the entire width between the pial surface and the ventricle, and a complex cell cycle which includes the translocation of the nucleus along the apical–basal axis by an interkinetic nuclear migration, giving rise to the pseudostratified structure of the neuroepithelium (Götz and Huttner, 2005). Neuroepithelial cells are firmly attached to the pia basal lamina by an endfoot, and previous studies have shown that dystroglycan and other proteins of the DGC are highly concentrated in these endfeet at the contact site to the basal lamina (Blank et al., 1997, 2002; Zaccaria et al., 2001). In this study we analyzed the function of the DGC in neuroepithelial cell endfeet *in vivo* using anti-dystroglycan antibodies, knockdown of dystroglycan synthesis with RNAi and overexpression of mutated dystroglycan cDNAs by *in ovo* electroporation. Our results show that dystroglycan is crucial for anchoring neuroepithelial cell endfeet to the basal lamina and for neuroepithelial cell morphology, proliferation and differentiation. Furthermore, our results also suggest that some of the brain abnormalities observed in some congenital muscular dystrophies might be caused by interfering with dystroglycan function at the endfoot–basal lamina interface.

Materials and methods

Animals

Fertile White Leghorn (*Gallus gallus domesticus*) chicken eggs were purchased from a local hatchery and incubated at 38 °C in a humid atmosphere. The age of the embryos was expressed as embryonic day (E) or according to the stages defined by Hamburger and Hamilton (HH; Hamburger and Hamilton, 1951). All experiments were conducted in accordance with the guidelines for the welfare of experimental animals issued by the Federal Government of Germany and the University of Mainz.

Cloning of chick dystroglycan

A cDNA coding for full-length chick dystroglycan was isolated from an embryonic chick muscle library by PCR using degenerate primers in combination with 5′RACE (System 2.0; Invitrogen, Karlsruhe, Germany). The 3′ end of chick dystroglycan was isolated from a COSMID (obtained from the German Research Center for Genome Research, RZPD, Heidelberg, Germany). The final cDNA had a length of 2933 base pairs (125 bp 5′-UTR, 117 bp 3′-UTR) and contained an open reading frame coding for 896 amino acids. The sequence was between 78% and 93% homologous to the corresponding sequences from rabbit, human, bovine, and mouse. In particular the predicted cleavage site between α- and β-dystroglycan at serine 655 was conserved (Esapa et al., 2003). The full-length sequence of chick dystroglycan has been deposited in the EMBL database (accession number: AM690436).

Antibodies and immunocytochemistry

The following primary antibodies were used: A monoclonal mouse anti-β-dystroglycan antibody (43DAG/8D5; Novocastra, Newcastle-upon-Tyne, UK), which recognizes 15 of the last 16 amino acids at the C-terminus of dystroglycan and cross-reacts with human, mouse, rat, bovine, rabbit and chick tissue; a monoclonal antibody against vimentin (VIM 3B4; Boehringer Ingelheim, Ingelheim, Germany); a monoclonal antibody against BrdU (clone Bu20a; DAKO Cytomation GmbH, Göttingen, Germany); a monoclonal antibody against acetylcholine esterase (AChE; mAb 3D10; Randall et al., 1987); a rabbit polyclonal antiserum against EGFP (Molecular Probes, Eugene, Oregon); a sheep polyclonal antiserum against the core protein of α-dystroglycan (Herrmann et al., 2000); a monoclonal antibody against the integrin β1-subunit (clone JG22; Sigma); a mouse monoclonal anti-utrophin antibody (mAb20C5; Bewick et al., 1992); a rabbit anti-α-dystrobrevin-1 antiserum (Blake et al., 1998); and a mouse anti-Ng-CAM monoclonal antibody (G4; Rathjen et al., 1987).

For light microscopy, embryonic chick tissues were immersion-fixed, sectioned and stained as described previously (Kröger, 1997). The primary antibodies were visualized using the appropriate secondary antibody conjugated to Alexa488 or Alexa594 fluorochromes, respectively, (Molecular Probes, Eugene, Oregon), as described (Blank et al., 1997). The nuclei were stained using bisbenzimide (Hoechst 33342 nuclear stain; Sigma) at a concentration of 10 μg/ml. Specimens were viewed using in a Leitz DMRA fluorescence microscope (63× oil immersion lens) equipped with a digital camera (DX 200; Leica, Solms, Germany) and an appropriate filter system for complete separation of both fluorochromes. Whole images were processed and contrast as well as brightness was adjusted using Adobe Photoshop (version 7.0, Adobe, Mountain View, CA, USA). Control sections stained with the secondary antibodies alone did not show any in specific immunoreactivity. Preabsorbed antisera were used to avoid cross reactivity between the secondary antibodies.

Polyclonal anti-dystroglycan antisera were generated in rabbits against a bacterially-expressed fusion protein of amino acid 564–749 or amino acid 555–749 inserted into the pET28a vector (Novagen, Madison, USA) and expressed in BL21 bacteria (Stratagene, La Jolla, USA). The vector contained a 6xHis epitope tag at the N- and C-terminus allowing affinity purification using the BugBuster- and the His-Bind Purification System (Novagen). The fusion protein appeared homogeneous as a single band after Coomassie blue staining. Two rabbits were immunized with each of the two purified fusion proteins. Sera were obtained after 175 days of immunization. The antisera were affinity-purified first using Protein A and then using the fusion protein coupled to sepharose-CL4B. Finally, Fab fragments were prepared from the affinity-purified IgG fraction using the ImmunoPure Fab-purification System (Pierce, Bonn, Germany). Fab fragments were dialyzed against PBS and concentrated using Centricon tubes (Amicon, Witten, Germany). All four antisera specifically detected α- as well as β-dystroglycan in Western blots of transfected cells and of muscle and brain tissue. Moreover, the antisera also stained the sarcolemmal plasma membrane in embryonic and adult muscle tissue, the inner limiting membrane and the outer plexiform layer of the retina, and the glia limitans and blood vessels in the entire CNS. Thus, the staining pattern obtained with these antisera was indistinguishable from the pattern described previously for α- and β-dystroglycan in muscle, retina and CNS tissue (Herrmann et al., 2000; Blank et al., 1997, 2002; Zaccaria et al., 2001), demonstrating that the antisera specifically detect dystroglycan.

The two fusion proteins used for immunization of the 4 rabbits contained the interaction site between α- and β-dystroglycan (Sciandra et al., 2001; Bozzi et al., 2001). The antisera were therefore tested if they inhibit the interaction between α- and β-dystroglycan *in vitro* using a co-immunoprecipitation assay. Fab fragments prepared from three out of the four antisera specifically inhibited the co-immunoprecipitation of the fusion protein with recombinantly expressed α-dystroglycan consistent with the idea that they inhibited the interaction between α- and β-dystroglycan (Figure S1 in supplementary material). These three independently prepared Fab fragments were subsequently used and gave identical results in all experiments.

The anti-dystroglycan Fab fragments were injected into the embryonic chick eye or tectum as described previously (Kröger et al., 1996). Between 0.2 and 1.9 μg (in a volume between 1 and 10 μl) of affinity-purified Fab fragments were injected once every day for 3 consecutive days between E4 and E9. Twenty-four hours after the final injection, embryos were sacrificed and the retina or tectum was dissected and analyzed. BrdU labeling of cells was performed by applying 100 μl of BrdU (10 mg/ml) for 3 h as described (Belecky-Adams et al., 1996).

Mutant dystroglycan cDNAs

Two mutant chick dystroglycan cDNAs were used in this study in addition to wild type dystroglycan (wt-dystroglycan) and the empty pMES vector. In one cDNA the cleavage site between the α- and the β-dystroglycan subunit was mutated by changing serine at position 655 to alanine (non-cleavable dystroglycan). This construct has been extensively characterized previously and shown to be transported to the plasma membrane and inserted in the appropriate orientation in transfected HEK293 cells (Esapa et al., 2003). Heterologous expression of this construct in HEK cells resulted in the synthesis of a protein with a molecular weight of 160 kDa as determined with an antibody against β-dystroglycan (Esapa et al., 2003). Likewise, expression of the construct in chick embryos by *in ovo* electroporation induced the synthesis of a β-dystroglycan-reactive protein of the same size, demonstrating the synthesis of dystroglycan in neuroepithelial cells as well as the absence of proteolytic processing of the mutated protein also in chick embryos *in vivo* (Figure S2 in supplementary material).

A second dystroglycan construct was generated by deleting the intracellular C-terminal most 15 amino acid of β-dystroglycan (truncated dystroglycan), and thus, removing the interaction site between β-dystroglycan and dystrophin or utrophin (Jung et al., 1995). This construct was generated using PCR and the following primers: DG-Δ15C-sense 5′-TCTAGAATGACTGTTG-GATGTGTCCCGCAGC-3′ and DG-Δ15C-antisense 5′-GGATCCCTAGATC-TTATCGTCGTCATCCTTGTAATCCATCGGGCGGGAGC-3′. The PCR reaction product was blunt-end cloned first into the pcDNA4/TO vector (Invitrogen, Karlsruhe, Germany). All dystroglycan constructs were then cloned into the bicistronic pMES vector (Swartz et al., 2001), that contains an internal ribosome entry site regulating the simultaneous expression of the gene of interest together with the enhanced green fluorescent protein (EGFP). This allowed the convenient distinction of transfected from untransfected cells. All constructs used in this study were routinely sequenced to eliminate the possibility of mutations.

In ovo electroporation

We used *in ovo* electroporation to analyze the function of dystroglycan *in vivo* during very early stages of CNS development. Microelectroporation of retinal neuroepithelial cells was performed as described previously (Momose et al., 1999). In short, 2 μg cDNA in approximately 0.5 μl PBS were injected into the optic stalk at E2 (HH stage 11). The left side of the embryo was then transfected by application of 5 square pulses of 15 V and 25 ms duration with 100 ms pulse interval using a BTX-830 pulse generator (BTX, San Diego, USA) in combination with a tungsten cathode (40 μm sharp tip), inserted into the ventricle through the neuropore, and a 5 mm gold electrode as anode placed laterally along the left side of the embryo. The chicken eggs were then sealed and further incubated for 1–5 days. Unless stated otherwise, embryos were examined 4 days after electroporation at E6. Analysis of the embryos showed that only the left side of the embryos was transfected and therefore the contralateral right side was always used as an internal control. Approximately 70% of the embryos were successfully transfected and in 50% of the embryos more than half of the retinal cells were transfected as determined by the presence of EGFP fluorescence.

RNAi knock-down of dystroglycan

Dystroglycan synthesis was inhibited posttranscriptionally using either long dsRNA or 21mer siRNA oligonucleotides followed by *in ovo* electroporation. Both approaches gave similar results. Long dsRNAi were generated by selecting three regions of the dystroglycan cDNA (two within the α-dystroglycan and one within the β-dystroglycan subunit) each with a length between 700 and 800 bp as targets and amplified using PCR and the following primers:

α-DG1-sense 5′-GCTCTAGAAGGACTTTGCTCCCAGTGC-3′;
α-DG1-antisense 5′-GGGGTACCTTCCACCACCTTCTTTGC-3′;
α-DG2-sense 5′-GCTCTAGAGAAGGCACTGGGACGGTC-3′;
α-DG2-antisense 5′-GGGGTACCGATGGTGCTGCTGTTCC-3′;
β-DG1-sense 5′-GTCCTAGAACCAACAACACCCTGC-3′ and
β-DG1-antisense 5′-GGGGTACCGGTCATGTTCTTCG-3′

The sequences covered different non-overlapping parts of the entire dystroglycan cDNA. The amplification products were cloned into the pSP72 vector (Promega, Mannheim, Germany) and single-strand RNAs were generated by *in vitro* transcription using the SP6 and T7 promoter according to the manufacturer's instructions (Promega). dsRNA was obtained by mixing equimolar amounts of the complementary single-strand RNAs and subsequent heating followed by slow cooling.

Since long dsRNAi might have unspecific effects and since their inhibitory effects are difficult to quantify due to the activation of the interferon-mediated apoptosis pathways, we repeated the experiments using two synthetic double-stranded small interfering RNA (siRNA) targeting dystroglycan (Qiagen, Hilden, Germany). The following dsRNA were used: siRNA-dag1 targeting

nucleotide 1560–1580 within the α-dystroglycan sequence: sense 5′r(AGGCCACGUUCAUUAAGAA)dTdT and antisense 5′r(UUGUCGUAGAAAGUAUCCG)dAdG; siRNA-dag2 targeting the β-dystroglycan sequence between nucleotide 2364 and 2384 sense 5′r(AGGCCACGUUCAUUAAGAA)dTdT and antisense 5′r(UUCUUAAUGAACGUGGCCU)dGdG. Two siRNAs were used as negative controls. siRNA-tmagrn1 (targeting nucleotide 5846 to 5866 of chick TM-agrin; Neumann et al., 2001) sense r(GGCUUUAUUGGCUGUAUAA)dTdT antisense r(UUAUACAGCCAAUAAAGCC)dAdG and siRNA-tmagrn2 (targeting nucleotide 880 to 900 of chick TM-agrin) sense r(GGACAAAUGCAAGGAUGAA)dTdT and antisense r(UUCAUCCUUGCAUUUGUCC)dAdG. The full-length dystroglycan and TM-agrin cDNAs were cloned into the psiCheck-2 vector (Promega, Madison, WI) and the inhibitory effect of the siRNAs on dystroglycan translation was determined using the Dual-Glo Luciferase Assay system (Kumar et al., 2003) according to the manufacturer's instructions (Promega). Luminescence was determined using a Veritas Microplate Luminometer (Turner Biosystems, Sunnyvale, CA). Both siRNA reduced dystroglycan expression to 20.6±1.8% (siRNA-dag1) and 23.1±5.6% (siRNA-dag2; mean±S.E.M. with $N=4$) of control values. Both siRNA targeting TM-agrin did not have an influence on dystroglycan expression, nor did the two siRNA targeting dystroglycan influence TM-agrin expression.

Injection of the RNAi and *in ovo* electroporation was performed in principle as described above. Approximately 0.5 μl containing 0.5 μg dsRNA were injected into a stage HH 11 chick embryo optic stalk. A single square pulse of 15 V and 25 ms was applied to transfect neuroepithelial cells selectively on the left side of the embryo. Cotransfection of the pMES vector, containing the EGFP expression cassette under the control of the chicken β-actin promoter, allowed the distinction of the transfected cells from untransfected cells.

All RNAi probes targeting dystroglycan reduced endogenous expression of α- and β-dystroglycan in the chick retina *in vivo* as determined by immunofluorescence using anti-dystroglycan antibodies and resulted in a thickened neuroepithel. None of the control RNAi probes had a detectable effect on dystroglycan expression and on the morphology of the neuroepithelium.

Results

Inhibition of dystroglycan function causes thickening of the neuroepithelium

As a first step to determine the function of dystroglycan in neuroepithelial stem cells, affinity-purified Fab fragments directed against the interaction site between α- and β-dystroglycan were injected daily for 3 consecutive days into the vitreous of live chick embryos. The injections were made between E5 and E9 since at this developmental stage, dystroglycan and the DGC are exclusively expressed by neuroepithelial cells and concentrated in their endfeet at the contact site to the inner limiting membrane (Blank et al., 2002), the basal lamina that separates the neural retina from the vitreous (Halfter et al., 1987). While injection of PBS, of the corresponding preimmune sera, or of the antisera in combination with an excess of the fusion protein used for immunization had no influence on the structure and overall appearance of the retina (Fig. 1A), injection of the affinity-purified anti-dystroglycan Fab fragments resulted in severe changes of the retinal morphology. The smooth surface of the retina–vitreous interface was lost and this was accompanied by an increase in radial thickness of the retina (Fig. 1B). The thickened retinal neuropil protruded into the vitreous humor but the contact between the retina and the pigment epithelium (dashed line in Figs. 1A, B) remained unaltered. Although the number of thickenings observed in injected retinae varied from experiment to experiment, we detected at least one affected area in more than 80% of the retinae analyzed.

We next injected the affinity-purified Fab fragments into the ventricle of the embryonic chick mesencephalon to determine if a similar change in the neuroepithelium could also be induced in other parts of the early developing CNS. While injection of PBS or of Fab fragments from the preimmune sera had no effect on the overall morphology of the tectal neuropil (Fig. 1C), injection of the affinity-purified Fab fragments induced an increase in the thickness of the mesencephalic neuroepithelium (Fig. 1D), demonstrating similar effects of the Fab fragments in the retina and in the tectum.

As an independent method to determine the role of dystroglycan in neuroepithelial cells *in vivo*, we inhibited the synthesis of dystroglycan using RNAi. Three non-overlapping dsRNA fragments of 700 to 800 bp length, two corresponding to the α-dystroglycan and one to the β-dystroglycan sequence, as well as two different siRNA (one targeting α-dystroglycan and one targeting β-dystroglycan) were injected into the optic vesicle of stage 11 embryos and transfected into neuroepithelial cells by *in ovo* microelectroporation (Momose et al., 1999). Transfected areas were identified by the co-electroporation of a plasmid coding for EGFP. The phenotypes obtained by RNAi transfection using the 5 different dsRNAs were indistinguishable with respect to both quality and penetrance. Electroporation of anti-α-dystroglycan (Fig. 1E) or anti-β-dystroglycan (Fig. 1F) RNAi resulted in an increased thickness of the neuroepithelial cell wall similar to that observed after injection of anti-dystroglycan Fab fragments. Staining with antibodies specifically against α- or β-dystroglycan (Figs. 1E, F, respectively) showed the severe reduction of dystroglycan immunoreactivity co-distributing with areas of increased neuroepithelial thickness. A similar phenotype was never observed after injection and electroporation of control dsRNA not targeting dystroglycan (see Materials and methods). In summary, our results indicate that inhibiting the interaction between α- and β-dystroglycan by Fab fragments or dystroglycan synthesis by RNAi induced an increase in the radial thickness of the neuroepithelial cell layer in the early developing CNS.

Altered morphology of neuroepithelial cells in thickenings

To investigate the morphology of neuroepithelial cells in more detail we stained sections of neuroepithelium with antibodies against vimentin, an intermediate filament protein expressed in neuroepithelial cells (Lemmon and Rieser, 1983). While in control tissues the anti-vimentin staining outlined the palisade-like radial structure of neuroepithelial cells with their processes in the pseudostratified neuroepithelium (Fig. 1G), this radial staining pattern was lost after Fab fragment injection (Fig. 1H) and the pattern of the anti-vimentin immunoreactivity appeared round or oval-shaped (compare Figs. 1G and H). A similarly altered staining pattern was observed in tecta that received Fab-fragment injections as well as in retinae treated with dystroglycan RNAi (see Figure S3 in supplementary material). Since the vimentin immunoreactivity reflects the overall shape of neuroepithelial cells, our results suggest that

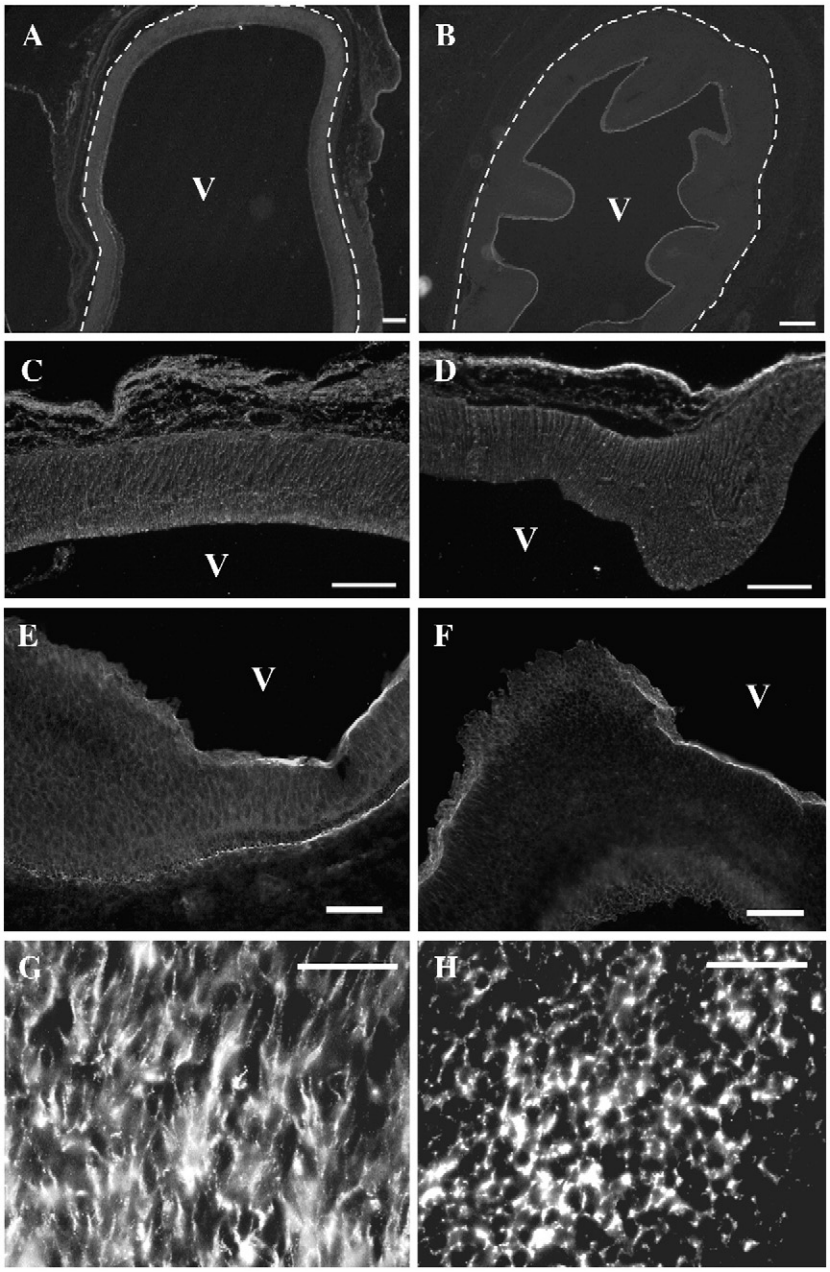

Fig. 1. Increase in radial thickness of the retinal and tectal neuroepithelium after anti-dystroglycan Fab fragment injection or RNAi electroporation. Cryostat sections of E9 retinal (A, B, E, F, G, H) or E7 tectal tissue (C, D) after injection of preimmune serum (A, C, G) or of affinity-purified anti-dystroglycan Fab fragments (B, D, H) into the vitreous (A, B, E, F) or into the mesencephalic brain ventricle (C, D) resulted in the formation of thickenings of the neuroepithelial cell wall. The thickenings developed by growth of the retina into the vitreous (V in panels A, B) or by growth of the tectum into the ventricle (V in panels C, D). The border between the retina and the pigment epithelium, marked by a dashed line in panels A and B, remained smooth. *In ovo* electroporation of anti-α-dystroglycan (E) or anti-β-dystroglycan (F) siRNA resulted in the formation of a similar increase in radial thickness of the neuroepithelium. To illustrate the spatially restricted influence of the RNAi, parts of the retina which were not affected are shown on the right side of panels E and F. Note the difference in the immunoreactivity of α-dystroglycan (panel E) and β-dystroglycan (panel F) co-distributing with the increased retinal thickness. Analysis of the vimentin staining at high magnification showed the altered morphology of neuroepithelial cells. While vimentin in neuroepithelial cells from control retinae had a radial distribution, spanning the width between pigment epithelium and vitreous (G), they had lost this palisade-like morphology after injection of the Fab fragments and the vimentin immunoreactivity appeared round or oval-shaped (H). Scale bar in panels A, B: 150 μm; C, D: 100 μm; E, F: 20 μm; G, H: 20 μm.

after interfering with dystroglycan interaction or synthesis neuroepithelial cells lose their radially oriented processes and adopt a more round or oval morphology.

The loss of the radial morphology of neuroepithelial cells after inhibition of dystroglycan interaction or synthesis together with the known concentration of dystroglycan in their endfeet suggested that the DGC might be involved in anchoring neuroepithelial cell endfeet to the basal lamina. To investigate this possibility, we transfected neuroepithelial cells by *in ovo* microelectroporation with constructs coding for mutated dystroglycan proteins. One construct had the C-terminal most 15 amino acids deleted, rendering the encoded dystroglycan

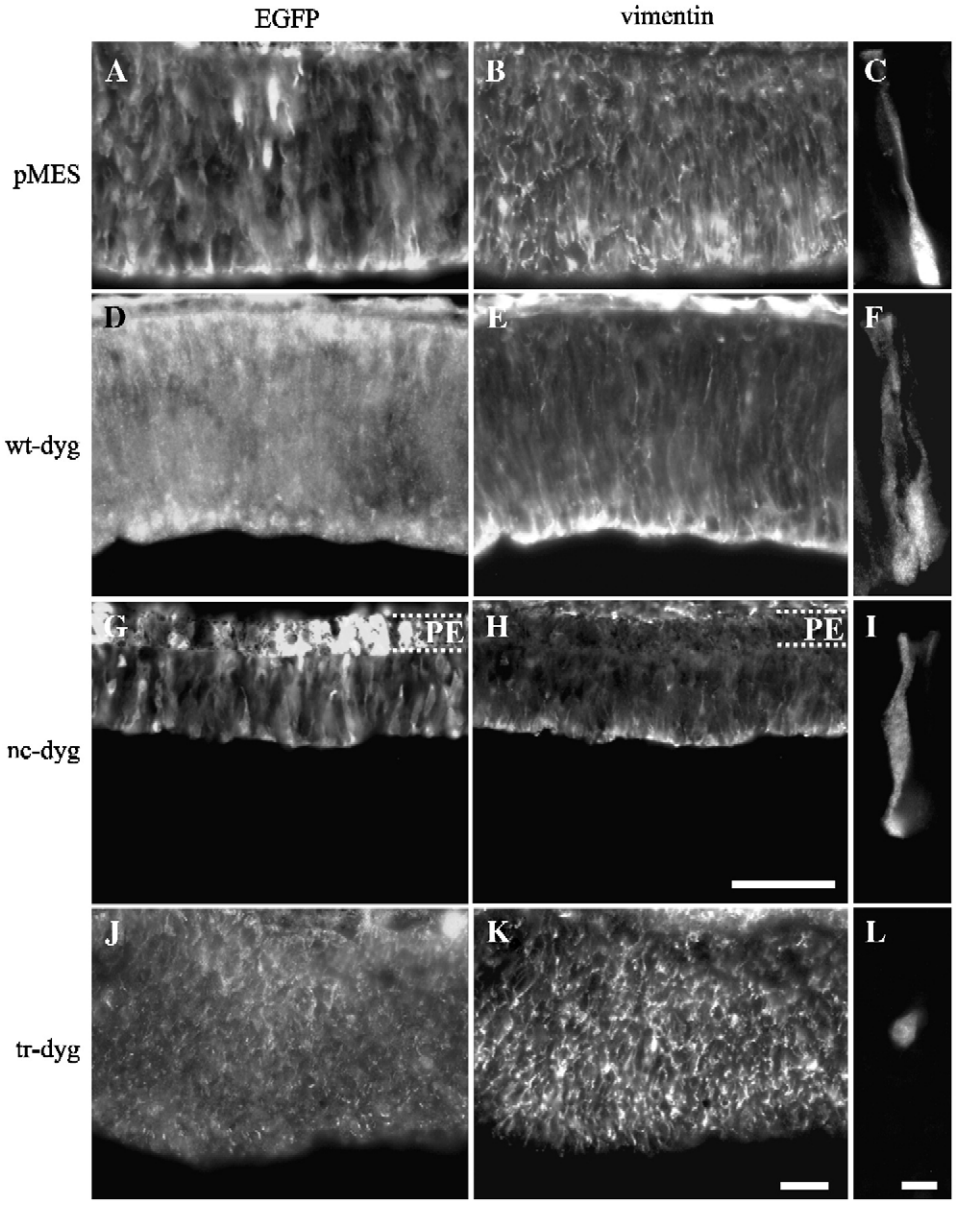

Fig. 2. *In ovo* electroporation of mutated dystroglycan constructs. Retinal neuroepithelial cells were transfected at E2 (HH stage 11) by *in ovo* microelectroporation with the empty pMES vector (A–C), or with the pMES vector containing wt-dystroglycan (wt-dyg; D–F), non-cleavable dystroglycan (nc-dyg; G–I) or truncated dystroglycan (J–L), respectively. The EGFP fluorescence of the transfected cells 4 days after transfection is shown in panels A, D, G, J and the vimentin staining of the same area is shown in panels B, E, H, K. A representative individual transfected neuroepithelial cell is shown in panels C, F, I, L. Note that the retina diameter is not affected by transfection of empty vector or wt-dystroglycan and that the neuroepithelial cells retain their radial morphology. Transfection of the non-cleavable dystroglycan construct resulted in a considerably thinner retina (compare panels G, H with A, B), although the overall radial morphology of the transfected neuroepithelial cells remained unaltered (panel I). In contrast, transfection of the truncated dystroglycan construct resulted in the loss of the radial structure of the transfected neuroepithelial cells, indicated by the round labeling after vimentin staining (panel K) as well as after analysis of the EGFP fluorescence of individual transfected cells at high magnification (panel L). Note that only a part of the affected retina is shown in panels J and K and that a lower magnification was used in these two panels. All panels are oriented with vitreal (basal) side of the neuroepithelium is facing down. The pigment epithelium (PE) is outlined by a dashed line in panels G and H. Scale bars in panels H and K: 50 μm; scale bar for C, F, I shown in L: 10 μm.

protein incapable of interacting intracellularly with dystrophin and utrophin. The other construct had a mutated proteolytic cleavage site so that the precursor protein could not be cleaved into the α- and β-dystroglycan subunit (Esapa et al., 2003). Both constructs were cloned into the pMES vector (Swartz et al., 2001) which contains an internal ribosomal entry site regulating the simultaneous expression of EGFP, allowing the discrimination of transfected from untransfected cells. While *in ovo* electroporation of empty pMES vector or pMES containing wild type dystroglycan did not influence the overall eye structure, electroporation of the non-cleavable construct significantly reduced the size of the eyes (2.1±0.9 mm compared to 3.4±0.5 mm in pMES or wt-dystroglycan treated retinae; mean eye diameter±S.E.M. with $N=3$; determined at E6, 4 days after electroporation). To investigate these changes in more detail, we analyzed the overall retinal structure and the

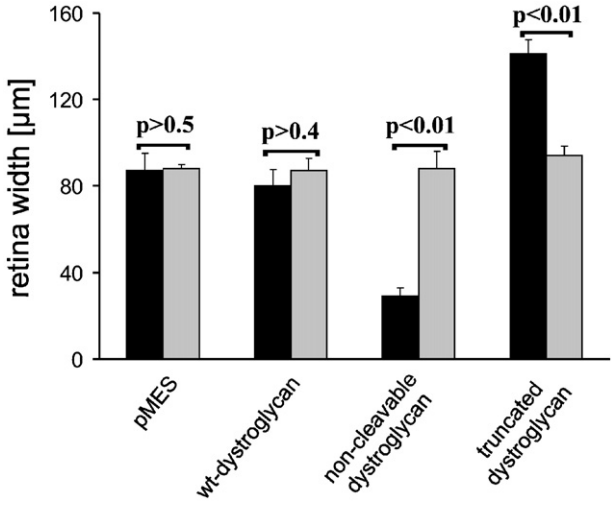

Fig. 3. Quantification of retina width after *in ovo* electroporation. The width of retinal areas transfected with either the empty vector (pMES), with vector containing wt-dystroglycan, non-cleavable dystroglycan or truncated dystroglycan, respectively, was determined (black bars) and compared to the width of the corresponding contralateral non-treated eyes of the same embryo (grey bars). The width of the retina of all contralateral eyes was similar to the width of eyes transfected with either empty vector or with vector containing the wt-dystroglycan, demonstrating that the transfection by *in ovo* electroporation itself had no effect on retinal structure. In contrast, the width of the retina was significantly reduced in regions transfected with non-cleavable dystroglycan and significantly increased in regions transfected with truncated dystroglycan. The values represent the mean ± S.E.M. from three independent experiments. Ten transfected areas were analyzed in each experiment. *P* values in two-tailed *t*-tests are indicated.

morphology of individual neuroepithelial cells after transfection with the different constructs. Fig. 2 shows parts of transfected retinae (indicated by the EGFP fluorescence; panels A, D, G, J) and the corresponding regions stained with anti-vimentin antibodies (B, E, H, K) to reveal the morphology of neuroepithelial cells. Expression of the empty pMES vector or of pMES containing wt-dystroglycan did not influence the overall retinal structure or the radial morphology of neuroepithelial cells (Figs. 2A, B, D, E). Transfection of the non-cleavable construct, however, resulted in a significant reduction of the width of the retinal neuroepithelium (Figs. 2G, H). In contrast, *in ovo* electroporation of the truncated dystroglycan construct increased retinal thickness and induced the formation of thickenings similar to those formed after Fab fragment injection and anti-dystroglycan RNAi treatment (Figs. 2J, K). Staining of areas transfected with the truncated dystroglycan construct using antibodies against vimentin also showed that the retinal neuroepithelium had lost its palisade-like pseudostratified structure and that neuroepithelial cells had lost their radial orientation and had developed a morphology similar to neuroepithelial cells treated with Fab fragments or anti-dystroglycan RNAi (compare Figs. 2B, E, H with K).

To investigate the morphology of transfected neuroepithelial cells in more detail, we analyzed the EGFP fluorescence of transfected neuroepithelial cells at high magnification. In order to analyze the morphology of individual cells we restricted our analysis to areas with a very low transfection rate. The right panels in Fig. 2 show representative individual cells transfected with empty pMES vector (panel C), wt-dystroglycan (panel F), non-cleavable dystroglycan (panel I), and truncated dystroglycan (panel L). Note that the EGFP fluorescence fills the entire neuroepithelial cells, including the processes. Neuroepithelial cells transfected with pMES, wt-dystroglycan or non-cleavable dystroglycan maintained their palisade-like radial structure and spanned the entire width between the inner limiting membrane and the ventricular (pigment epithelium) side. However, the length along the apical-basal axis of the neuroepithelial cells transfected with the non-cleavable construct was significantly reduced (Fig. 2I), most likely explaining the decreased eye size observed after transfection of non-cleavable dystroglycan. In contrast, all neuroepithelial cells transfected with the truncated dystroglycan construct appeared round in EGFP fluorescence analysis as indicated in Fig. 2L which shows one representative cell out of a group of several labeled cells within a single section. These data support the hypothesis that inhibition of the interaction between α- and β-dystroglycan, inhibition of dystroglycan synthesis, or expression of truncated dystroglycan results in the loss of the radial structure of neuroepithelial cells.

To quantify these changes, the thickness of transfected retinal areas (indicated by the EGFP fluorescence) was determined (black bars in Fig. 3) and directly compared to the retinal thickness of the contralateral non-transfected eye (grey bars in Fig. 3). While *in ovo* electroporation of wt-dystroglycan or of the empty pMES vector had no effect on the width of the

Fig. 4. Mutated dystroglycan expression influences neuroepithelial cell proliferation. To analyze the proliferation of neuroepithelial cells, retinae were transfected at HH stage 11 with either the empty pMES vector (A, E, I), vector containing wt-dystroglycan (wt-dyg; B, F, J), non-cleavable dystroglycan (nc-dyg; C, G, K) or truncated-dystroglycan (tr-dyg; D, H, L), respectively, and analyzed 4 days later at E 6. Proliferating cells were marked by a 3-h pulse of BrdU. The cells in transfected areas were subsequently analyzed using the EGFP fluorescence (A–D), bisbenzimide staining (E–H) and antibodies against BrdU (I–L). Nuclei labeled by BrdU were primarily localized at the vitreal side of the retina (labeled by a dashed line in panels C, G, K and N) in neuroepithelial cells transfected with empty vector, with wt-dystroglycan, or with the non-cleavable dystroglycan (panels I, J, and K, respectively). However, considerably less BrdU-labeled cells were observed after transfection with the non-cleavable construct (compare panel K with I and J). Moreover, a significant increase in the number of BrdU-labeled cells was observed after transfection with the truncated dystroglycan construct (compare panel L with I and J). The results were quantified by determining the percent of BrdU-labeled cells per total number of cells in 100 µm segments of retinae (panel M), either transfected with the indicated cDNA (black bar) or of non-transfected contralateral control retinae (grey bar). The values represent the mean ± S.E.M. with $N=3$ in all experiments. *P* values for two-tailed *t*-tests are indicated. Ten segments were analyzed in each experiment. Panel N shows a high magnification of panel G to illustrate the concentration of nuclei at the vitreal side (marked by a dashed line in panels G and N) and their absence from the apical side of the retina after transfection with the non-cleavable dystroglycan construct. Note that parts of the pigment epithelium (PE) is shown in panels C, G, and N. Panels O and P show bisbenzimide-labeled nuclei after transfection with wt-dystroglycan (O) and with truncated dystroglycan (P) to illustrate their oval and round morphology, respectively. The vitreal (basal) side of the retina is at the bottom of each panel. Note that a lower magnification was used in panels D, H, and L compared to panels A–K, respectively. Scale bar A–N: 100 µm; O, P: 20 µm.

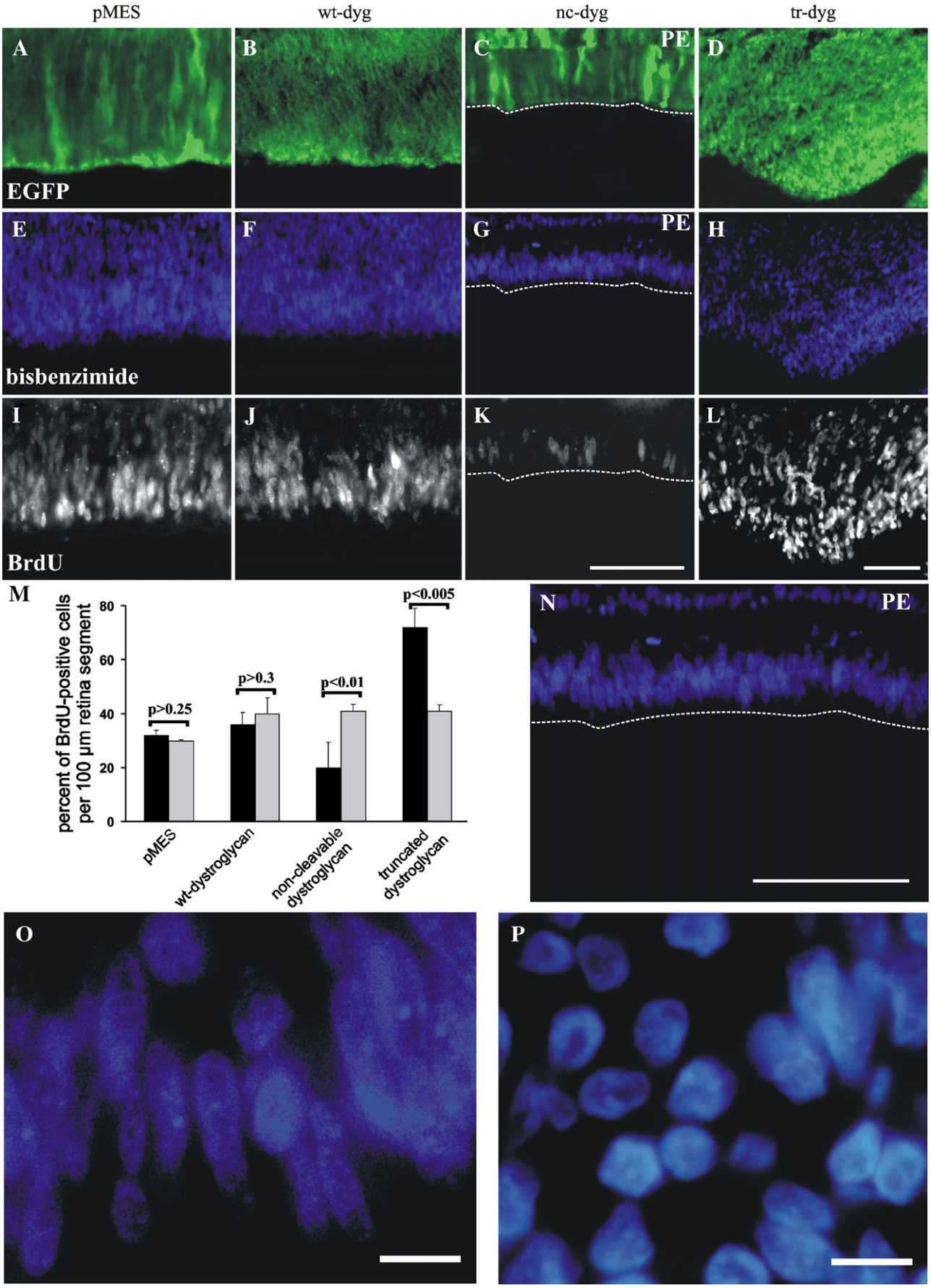
pMES
wt-dyg
nc-dyg
tr-dyg
A
B
C
PE
D
EGFP
E
F
G
PE
H
bisbenzimide
I
J
K
L
BrdU
M
percent of BrdU-positive cells per 100 µm retina segment
80
60
40
20
0
p>0.25
p>0.3
p<0.01
p<0.005
pMES
wt-dystroglycan
non-cleavable dystroglycan
truncated dystroglycan
N
PE
O
P

neuroepithelium, transfection with the non-cleavable construct reduced the thickness to approximately one-third of control values, while transfection with the truncated dystroglycan cDNA had the opposite effect and increased the thickness of the retina by approximately 50%.

Increase of retinal radial thickness result from hyperproliferation of neuroepithelial cells

To analyze if the increased width of the retina was the result of an increased proliferation of neuroepithelial cells, we labeled dividing cells 4 days after electroporation by a 3-h pulse of BrdU and subsequent staining with anti-BrdU antibodies. As shown in Fig. 4, BrdU-labeled nuclei were localized primarily at the vitreal side of retinae transfected with pMES or with wt-dystroglycan (Figs. 4I, J). We observed an increased number of BrdU-labeled cells after electroporation of the truncated dystroglycan construct and these cells were localized throughout the retinal width (Fig. 4L). Likewise, intraocular injection of anti-dystroglycan Fab fragments lead to an increase in number and to a more widespread distribution of the BrdU-labeled cells. In contrast, electroporation of the non-cleavable dystroglycan construct reduced the number of BrdU-labeled neuroepithelial cells (Fig. 4K). These results were quantified by comparing the percentage of BrdU-labeled cells with the total number of cells (as determined by bisbenzimide nuclear staining; Figs. 4E–H) within 100 μm retina segments (black bars in Fig. 4M). The contralateral untreated eyes served as controls (grey bars in Fig. 4M). The quantification demonstrated that 4 days after transfection the number of BrdU-labeled cells was almost doubled in areas transfected with truncated dystroglycan and reduced to almost half after electroporation of the non-cleavable dystroglycan. Similar results were obtained after intravitreal injection of anti-dystroglycan Fab fragments (93 ± 13.5 BrdU-labeled cells, compared to 53 ± 11.1 cells in preimmune serum-injected retinae; mean ± S.E.M. with $N = 3$; analysis at E9 4 days after first Fab fragment injection) and after injection of the Fab fragments into the ventricle of the mesencephalon (99 ± 4.6 cells labeled by anti-BrdU antibodies in 100 μm segments after injection of the preimmune serum compared to 45 ± 5 cells in control retinae; mean ± S.E.M. with $N = 3$; analysis at E7, 3 days after first Fab fragment injection). These results demonstrate that the increased thickness of the neuroepithelium after transfection with the truncated dystroglycan construct or after Fab fragment injection is due to an increased proliferation of neuroepithelial cells. Moreover, the decrease in neuroepithelial cell proliferation after electroporation of the non-cleavable dystroglycan construct suggests an essential role for the post-translational processing of dystroglycan in the regulation of the cell cycle of neuroepithelial cells. The reduced proliferation rate is most likely also the explanation for the reduced size of eyes transfected with the non-cleavable dystroglycan construct.

Interestingly we noted that the nuclei of neuroepithelial cells transfected with non-cleavable dystroglycan were not evenly distributed throughout the width of the retina, but instead had accumulated at the vitreal (basal) side (Fig. 4N). Together with the observed reduced proliferation rate, this result suggests that the interkinetic migration of the nucleus of cells expressing the non-cleavable dystroglycan was inhibited at a particular position and that the cell cycle of neuroepithelial cells was not able to progress beyond a particular phase. Furthermore, electroporation with the truncated dystroglycan construct also influenced nuclear morphology. While control cells transfected with pMES, wt-dystroglycan, or non-cleavable dystroglycan had an oval shaped nucleus, nuclei of cells transfected with the truncated dystroglycan construct were round (compare bisbenzimide staining in Figs. 4O and P). Thus, the treatments that resulted in the loss of the radial structure of the neuroepithelial cells also changed the morphology of the nuclei.

Previous studies had shown that impaired dystroglycan function results in the formation of ectopias, heterotopias and other CNS abnormalities due to a fragmented basal lamina (glia limitans; Moore et al., 2002; Saito et al., 1999; Kurahashi et al., 2005; Lee et al., 2005). To rule out the possibility that the increased thickness of the retinal and tectal neuroepithelium developed due to a ruptured basal lamina, we determined the integrity of the inner limiting membrane of the retina after *in ovo* electroporation of wt- and mutated dystroglycan cDNA by staining with antibodies against agrin and laminin. We found no evidence for basal lamina fragmentation in retinae transfected with any of the dystroglycan constructs (Figure S4 in supplementary material). Likewise, we did not observe basal lamina fragmentation in eyes or tecta treated with the anti-dystroglycan Fab fragments (data not shown). These results demonstrate that the increase in retinal and tectal thickness and the increased number of neuroepithelial cells were not the result of a fragmented basal lamina.

Dystroglycan influences neurogenesis

To determine if the increased proliferation observed after inhibition of dystroglycan interaction or synthesis as well as

Fig. 5. Neurogenesis is altered after transfection of dystroglycan constructs. The EGFP fluorescence (panels A–D), bisbenzimide nuclear staining (panels E–H), and AChE staining for postmitotic neurons (panels I–L) in cryostat sections of E6 retinae transfected at E2 with either empty vector (pMES; A, E, I), wt-dystroglycan (wt-dyg; B, F, J), non-cleavable dystroglycan (nc-dyg; C, G, K) or truncated dystroglycan cDNA (tr-dyg; D, H, L) are shown. All panels are oriented with the vitreal (basal) side facing down. While under control conditions retinal AChE-positive postmitotic neurons (representing retinal ganglion cells) were localized in a single layer at the vitreal border of the retina, AChE-labeled cells were more numerous and had a more widespread distribution in retinae transfected with the truncated dystroglycan construct (compare panels I, J with panel L). In contrast, very few if any AChE-labeled cells could be detected in retinae transfected with the non-cleavable dystroglycan construct (panel K). Quantification of these results is shown in panel M. The percentage of AChE-labeled cells per total number of cells in a 100 μm section was determined in retinae transfected with the indicated constructs (black bars) and compared to the corresponding non-transfected contralateral retina (grey bars). The values represent the mean ± S.E.M. with $N = 3$ in all cases. P values for two-tailed t-tests are indicated in panel M. Note that a smaller magnification was used in panels D, H, L. Scale bars in panels I and L: 100 μm.

after transfection of truncated dystroglycan was accompanied by an increase in neuronal differentiation, we stained treated retinae with antibodies against acetylcholine esterase (AChE). AChE has previously been shown to be a marker for postmitotic neurons in the developing chick CNS (Layer and Sporns, 1987). In retinae transfected with either pMES alone (Figs. 5A, E, I) or with pMES containing wt-dystroglycan (Figs. 5B, F, J) post-mitotic neurons were found in a single layer (ganglion cell

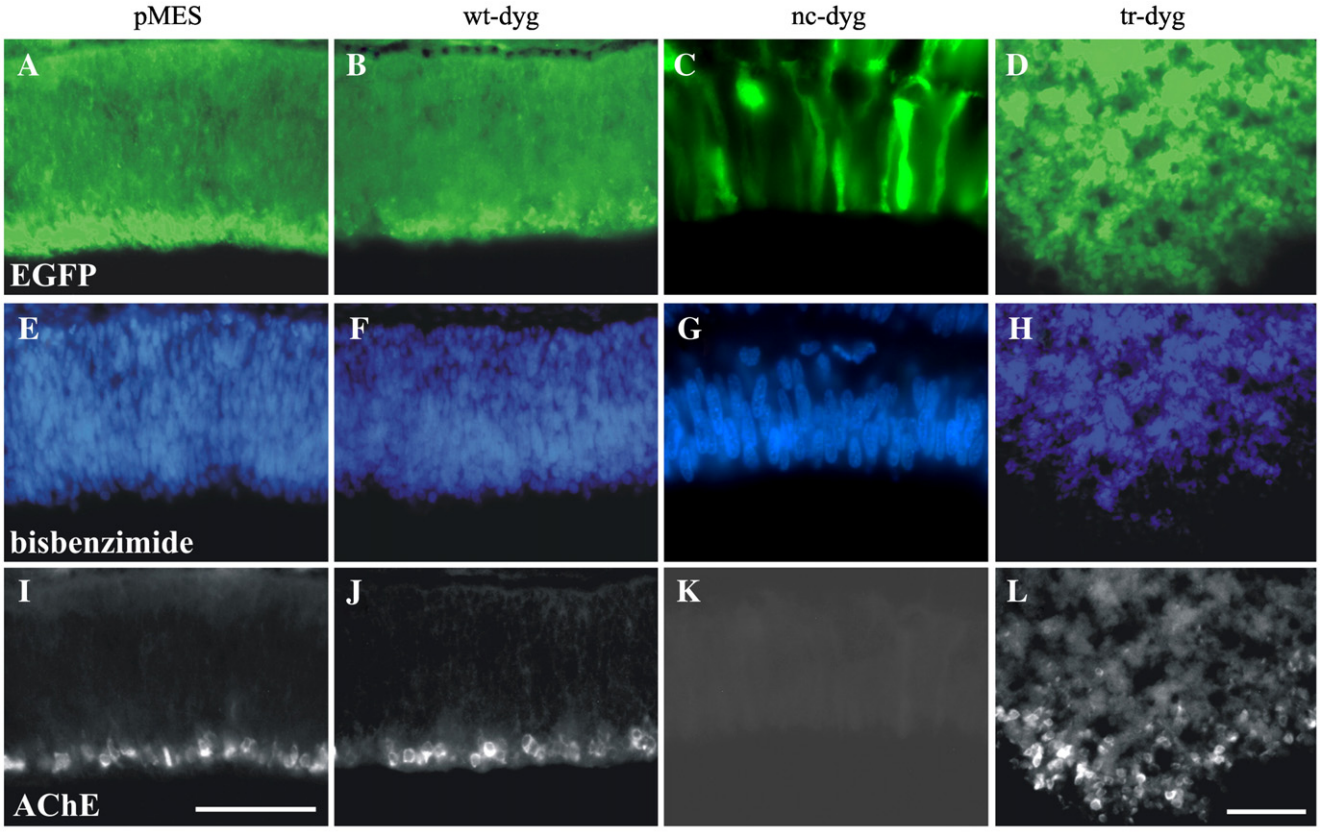

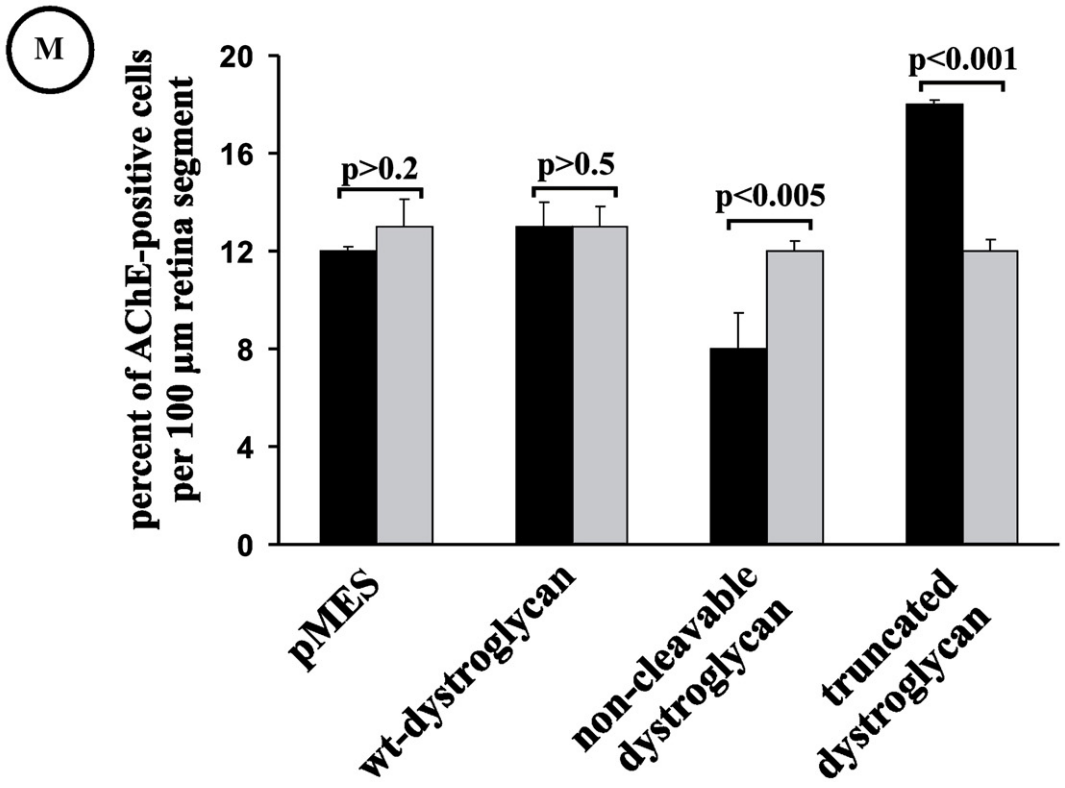

layer; GCL) at the border between retina and vitreous. On the other hand, transfection of non-cleavable dystroglycan resulted in the differentiation of significantly less postmitotic neurons, with large areas of the retina apparently without AChE immunoreactivity (Figs. 5C, G, K). In contrast, retinae transfected with the truncated dystroglycan construct had many more AChE-positive cells compared to control retinae, suggesting an increased neuronal differentiation of neuroepithelial cells. However, the AChE-positive cells were not concentrated at the vitreal border of the retina but instead found throughout the retinal neuropil (Figs. 5D, H, L). These results were quantified by determining the percent of AChE-positive cells per total number of cells (determined by bisbenzimide staining) in 100 μm wide retinal segments (black bars in Fig. 5M) and comparing this number to the percent of labeled cells in the contralateral, non-treated retina of the same embryo (grey bars in Fig. 5M). While transfection of empty pMES vector or of wt-dystroglycan had no effect on the number of AChE-positive cells, the number of labeled cells was reduced by approximately one-third after transfection with the non-cleavable dystroglycan construct and increased by approximately one-third after transfection with the truncated dystroglycan construct (Fig. 5M). Similar differences were observed when anti-Thy-1 antibodies or anti-neurofilament NF68 antibodies were used to label postmitotic neurons or their neurites (data not shown). Moreover, we found a similar increase in the number of postmitotic neurons after Fab fragment injection into the vitreous of the eye (data not shown) or into the ventricle of the mesencephalon (Figure S5 in supplementary material). In summary, our results demonstrate that inhibition of dystroglycan interaction by Fab fragments, or of dystroglycan synthesis by RNAi, or overexpression of the truncated dystroglycan construct resulted in the differentiation of more postmitotic neurons in the retina and in the tectum. These neurons were however ectopically localized and did not accumulate in the appropriate layer. In contrast, expression of the non-cleavable dystroglycan protein severely reduced the number of postmitotic neurons.

Distribution of basally concentrated proteins

To determine if interfering with dystroglycan function had an influence on proteins concentrated in the endfeet, we stained neuroepithelial cells transfected with the different dystroglycan constructs using a number of antibodies against basally concentrated proteins, including other components of the DGC. Utrophin has been shown to interact with dystroglycan in skeletal muscle and to be concentrated in the endfeet of neuroepithelial cells (Blank et al., 2002). Staining of retinal neuroepithelial cells transfected with pMES or with pMES containing wt-dystroglycan confirmed the concentration of utrophin at the vitreal border of the retina (Fig. 6A). In contrast, utrophin immunoreactivity was reduced at the retina–vitreous interface in eyes transfected with the non-cleavable construct (Fig. 6D). Likewise, staining intensities with antibodies against α-dystrobrevin-1 or against β1-integrin in neuroepithelial cell endfeet were significantly reduced in regions transfected with non-cleavable dystroglycan (Figs. 6E, F), compared to cells transfected with wt-dystroglycan. In contrast, we found a redistribution of utrophin, α-dystrobrevin-1 and β1-integrin in cells transfected with the truncated dystroglycan (Figs. 6G, H, I). All proteins were detectable in a much broader area, and the immunoreactivities were not strictly concentrated at the border between retina and vitreous. Likewise, staining of cells transfected with the truncated dystroglycan construct using an antibody against the last 15 amino acids of β-dystroglycan (which only labels endogenous dystroglycan, since this epitope is missing in the transfected truncated dystroglycan protein), showed a loss of the polarized distribution of endogenous β-dystroglycan in the transfected cells (data not shown). All changes were restricted to the transfected areas (identified by EGFP fluorescence) and not observed in untransfected areas of the same tissue. In summary, the results show that the subcellular concentration of the DGC and of other proteins in the endfeet of neuroepithelial cells was severely compromised in neuroepithelial cells transfected with the truncated- or with the non-cleavable dystroglycan construct.

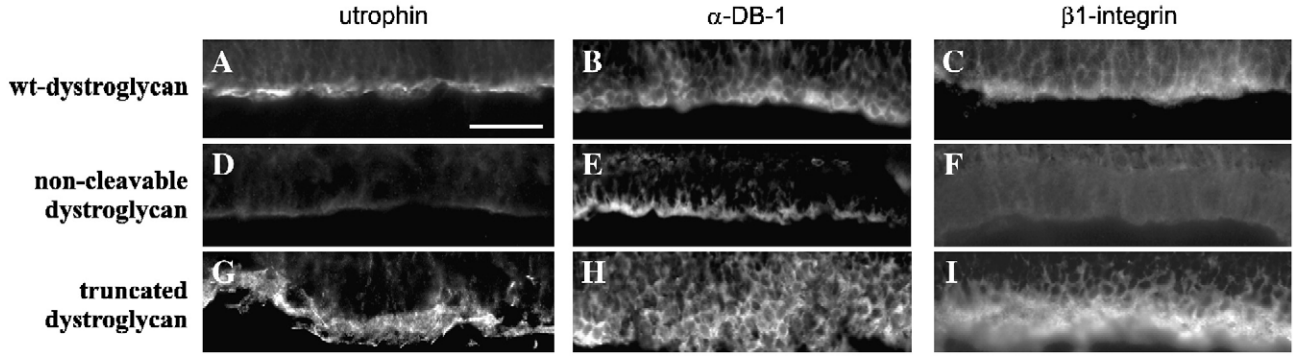

Fig. 6. Distribution of basally concentrated proteins in neuroepithelial cells after transfection of the dystroglycan constructs. Cryostat sections of E6 retinae transfected with wt-dystroglycan (panels A–C), non-cleavable (D–F) and truncated dystroglycan (G–I) were stained with antibodies against utrophin (panels A, D, G), α-dystrobrevin-1 (α-DB-1; panels B, E, H) and β1-integrin (panels C, F, I). Similar exposure times were used in all cases. Note the reduced immunoreactivity with all three antibodies in retinae transfected with non-cleavable dystroglycan (panels E, F) and the widespread distribution of the three proteins in retinae transfected with the truncated dystroglycan construct (panels G, H, I). Scale bar in panel A: 20 μm.

Impaired dystroglycan function in neuroepithelial cells alters axonal growth

Our results so far suggested that interfering with dystroglycan function or synthesis caused a loss of the radial morphology of neuroepithelial cells and the loss of specializations at the contact site of their endfeet to the basal lamina. Since the endfeet, in addition to anchoring neuroepithelial cells to the basal lamina, also provide guidance cues for growing axons, we reasoned that the loss of the radial morphology and the loss of the endfeet basal lamina attachment might influence axonal orientation. We therefore investigated the orientation of axonal growth in retinae transfected with the various constructs. Fig. 7 shows areas of flat-mounted retinae 3 days after electroporation at low (panels A–D) and at high magnification (panels E–H) stained with an antibody against Ng-CAM, a cell adhesion molecule which is expressed on all long-distance projecting neurons and which in the retina and tectum labels the axons of postmitotic neurons without staining of their cell bodies (Halfter et al., 1987; Kröger and Schwarz, 1990). In non-transfected retinae or retinae transfected with pMES, axons of retinal ganglion cells grew centripetally in almost-parallel fascicles towards the exit of the optic nerve head (Figs. 7A, E). This overall pattern was maintained in retinae transfected with wt-dystroglycan or with non-cleavable dystroglycan (Figs. 7B, F, C, G). In contrast, expression of truncated dystroglycan dramatically altered the orientation of retinal ganglion cell axons (Figs. 7D, H). In the transfected areas (indicated by an asterisk in Fig. 7D) we observed a complete loss of the centripetal growth, and a random orientation of the axons. A similar loss of orientation was observed in retinae treated with anti-dystroglycan RNAi (data not shown). Moreover, tectobulbar axons in the mesencephalon (Kröger and Schwarz, 1990) lost their ventrally oriented growth after injection of the affinity-purified anti-dystroglycan Fab fragments into the mesencephalic ventricle (Figure S6 in supplementary material), demonstrating that the loss of the orientation after interfering with dystroglycan function could also be observed in other parts of the developing CNS. Moreover, since dystroglycan is not expressed by growing retinal or tectal axons, these data suggest a non cell autonomous mechanism via altered neuroepithelial cells.

Discussion

Dystroglycan and other proteins of the DGC are highly concentrated in the endfeet of neuroepithelial cells throughout the CNS (Blank et al., 2002; Zaccaria et al., 2001; Luniardi et al., 2006). Since one function of the DGC in skeletal muscle is the formation of a molecular bridge between the cytoskeleton and the basal lamina and to provide a scaffold for the attachment of proteins, we hypothesized that it might play similar roles in neuroepithelial cells of the developing CNS. Here we show that interfering with dystroglycan function in neuroepithelial cells *in vivo* by injection of anti-dystroglycan Fab fragments, inhibition of dystroglycan synthesis or expression of a truncated dystroglycan cDNA results in the loss of their radial morphology, in hyperproliferation with subsequent thickening of the neuroepithelium, and in an increased number of postmitotic

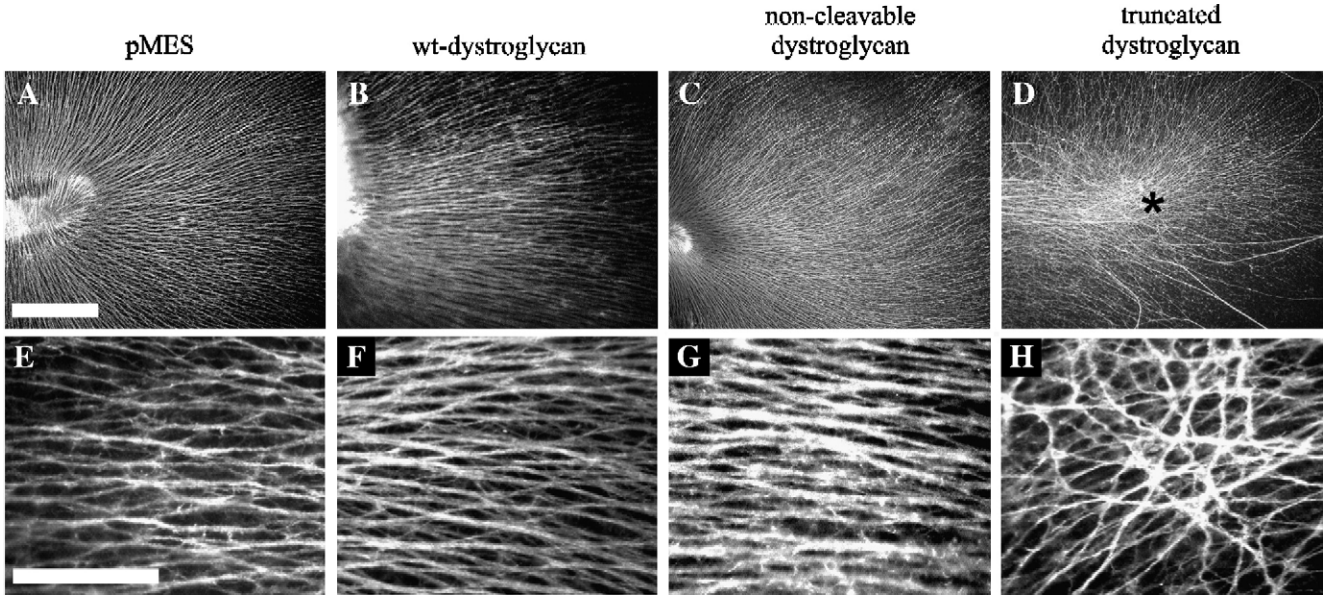

Fig. 7. Altered axonal growth after transfection of truncated dystroglycan. Flat-mounted E6 retinal wholemounts were labeled with antibodies against NgCAM and shown at low (panels A–D) and at high (panels E–H) magnification. Transfection of retinae with the empty vector (pMES; A, E), wt-dystroglycan (B, F) or non-cleavable dystroglycan (C, G) did not influence the directionality of retinal ganglion cell axon growth. Although we observed a slightly increased number of axons switching between the fascicles in areas transfected with the non-cleavable construct (compare panels E and G), the overall orientation of growth was directed towards the optic fissure and the exit of the optic nerve (located on the left side in panels A–D). In contrast, this centripetal orientation was lost in retinae transfected with the truncated dystroglycan construct (panels D and H). The fascicles were oriented in all directions and many axons failed to reach the optic nerve and to exit the eye. Note that the loss of oriented axonal growth was only local and restricted to the area affected by the transfection. Scale bar in panels A: 200 μm; E: 100 μm.

neurons. In contrast, overexpression of non-cleavable dystroglycan in neuroepithelial cells had the opposite effect, i.e. a reduced thickness of the neuroepithelium, less proliferation, and a reduced number of differentiated postmitotic neurons. In summary, these data demonstrate a key role for dystroglycan in neuroepithelial cell structure, proliferation and differentiation.

Neuroepithelial cells are multipotent precursor cells for neurons and glial cells of the CNS (for review see Kriegstein and Götz, 2003; Götz and Huttner, 2005). Neuroepithelial cells have a radial morphology and span the entire width of the neuroepithelium extending from the lumen of the ventricle to the pial surface via processes. They are polar cells with an apical (ventricular) and a basal (pial) side (for review see Götz and Huttner, 2005). Both sides are molecularly, morphologically and functionally specialized. For example, at their basal side neuroepithelial cells have a process with an endfoot at its tip, which anchors the cell to a basal lamina (glia limitans in the brain or inner limiting membrane in the retina) and, thus, maintains the radial morphology. The radial structure of neuroepithelial cells is important for at least two processes: The neuroepithelial cell nucleus undergoes an interkinetic migration, translocating within the cell between the ventricular and the pial surface. Different stages of the cell cycle are correlated with specific positions of the nucleus during this translocation (Sauer, 1935; Götz and Huttner, 2005). The radial morphology of neuroepithelial cells and a polarized cytoskeleton are necessary for the translocation of the nucleus. In addition, the radial structure of the neuroepithelial cells is required for the migration of differentiated neuroblasts to their appropriate layer (for review see Kriegstein and Noctor, 2004).

In this study we provide several lines of evidence for a fundamental role of dystroglycan in maintaining the radial morphology of neuroepithelial cells *in vivo*: First, interfering with the interaction between α- and β-dystroglycan by injection of affinity-purified anti-dystroglycan Fab fragments, or inhibition of dystroglycan synthesis using RNAi or overexpression by *in ovo* electroporation of a dystroglycan construct which lacks the C-terminal most 15 amino acid and, thus, is incapable of interacting with dystrophin or utrophin, lead to a loss of the radial morphology of neuroepithelial cells and to the development of a round or oval shape. Second, the same treatments also changed the shape of the nuclei from elongated to round, suggesting that the apically–basally oriented cytoskeleton was not able to form or to maintain the radial structure of neuroepithelial cells and their nuclei. Third, the polarized distribution of several proteins, including utrophin, β1-integrin and α-dystrobrevin-1, was altered from being highly concentrated in the endfeet to a broader distribution. Fourth, these different treatments also affected the orientation of axons that use endfeet-derived signals to navigate towards their target tissue, consistent with the idea that the processes and their endfeet were not present under these conditions. Finally, postmitotic neurons were found widely dispersed within the retina and tectum, suggesting that migration of postmitotic neurons into the appropriate layer was compromised. In summary, our data support the hypothesis that in endfeet of neuroepithelial cells dystroglycan and the DGC form a molecular connection between the cytoskeleton and the basal lamina and that interfering with dystroglycan function or synthesis detaches the endfoot from the basal lamina resulting in an altered cytoskeleton, in a loss of the radial structure, and in a loss of the polarized distribution of basally concentrated proteins.

Why does transfection of the truncated dystroglycan result in the same structural changes of neuroepithelial cells as inhibition of dystroglycan interaction by Fab fragments or inhibition of dystroglycan synthesis? One possibility is that the lack of the intracellular interaction site interrupts the connection between extracellular matrix and cytoskeleton, resulting in the loss of adhesion between the neuroepithelial cell endfoot and the basal lamina. However, an alternative and possibly more likely explanation might be that the lack of the intracellular interaction domain of β-dystroglycan with dystrophin and utrophin does not allow the post-translational assembly of the DGC and interferes with the polarized transport of the complex to the endfeet. Previous studies in skeletal muscle and CNS tissue have demonstrated that mutations in individual components of the DGC influence the assembly of the complex, leading to an absence or redistribution of most if not all other DGC proteins from the plasma membrane (see for example Cohn et al., 2002; Lee et al., 2005). We suggest that a similar mechanism applies to neuroepithelial cells. In agreement with this possibility we show that several DGC components, normally concentrated in the neuroepithelial cell endfeet, including endogenous β-dystroglycan, utrophin, and α-dystrobrevin-1, have an altered distribution in cells transfected with truncated dystroglycan. Thus, our results suggest that in neuroepithelial cells truncated dystroglycan acts in a dominant-negative manner by interfering with the assembly and subcellular concentration of the DGC in neuroepithelial cell endfeet.

Previous studies have demonstrated that integrins are important for the adhesion of neuroepithelial cell endfeet to the basal lamina. For example, CNS-specific deletion of the β1-integrins in transgenic mice resulted in a loss of glial cell endfeet anchorage, altered meningeal basement membrane formation and, as a consequence, altered cortical lamination (Graus-Porta et al., 2001; Haubst et al., 2006). In this study we provide evidence that dystroglycan is also involved in the adhesion of neuroepithelial cell endfeet to the basal lamina raising the possibility that in the developing CNS both proteins might have overlapping functions or might influence each other. Several studies have suggested a functional influence of integrins on the dystrophin associated protein complex (see for example Burkin et al., 2001; Cerna et al., 2006). In agreement with this we show that the distribution of β1-integrins in retinae treated with RNAi or with affinity-purified Fab fragments, or transfected with the truncated dystroglycan construct was altered, suggesting that dystroglycan is able to influence β1-integrin distribution in endfeet of neuroepithelial cells. It remains to be determined, however, if this is a direct consequence of the dystroglycan loss of function, or an indirect, caused for example by the loss of the endfeet and the subsequent lack of basal specializations.

In addition to the altered morphology, interfering with dystroglycan function or synthesis also induced hyperprolifera-

tion of neuroepithelial cells and subsequently the formation of thickenings in the retina and tectum. Conversely, rendering the interaction between α- and β-dystroglycan permanent by expression of non-cleavable dystroglycan reduced the width of the neuroepithelium and the number of proliferating cells, demonstrating that dystroglycan influences the proliferation of neuroepithelial cells in the developing brain. Concomitant with the hyperproliferation we observed a change in the morphology of the nuclei from oval/elongated to a round shape. Since an elongated shape is typical for nuclei during interkinetic nuclear migration, whereas a round morphology is adopted when migration has stopped (Haubensak et al., 2004), this result supports the idea that interfering with dystroglycan function or synthesis influences neuroepithelial cell proliferation. In agreement with this hypothesis, mice with a GFAP promoter-mediated brain-specific deletion of dystroglycan showed an increase in brain weight of approximately 20% without simultaneous increase in body weight (Moore et al., 2002). It remains to be determined however, how dystroglycan influences neuroepithelial cell number. One possibility to explain the altered proliferation would be an increase or decrease in apoptosis. However, we did not observe fragmented nuclei or pycnotic cells after transfection of the mutated dystroglycan constructs or after Fab fragment injection, making this possibility rather unlikely. It appears more likely that similar to the role of the DGC in skeletal muscle inhibition of dystroglycan function detaches the endfeet from the basal lamina and disrupts the neuroepithelial cell polarity. Dystroglycan has been shown to be important for the polarity of epithelial cell (Durbeej et al., 1995, 2001; Muschler et al., 2002; Deng et al., 2003; Shcherbata et al., 2007). In analogy, interference with dystroglycan function in neuroepithelial cells might lead to a loss of their polarity with a subsequently altered proliferation. However, since neither the CNS-specific deletion of β1-integrin (Graus-Porta et al., 2001; Haubst et al., 2006), nor the removal of the pia basal lamina by either genetic means (Halfter et al., 2002) or by collagenase injection (Halfter and Schurer, 1998) resulted in a phenotype similar to the one described in our study, the simple mechanical detachment of the neuroepithelial cell endfeet from the basal lamina alone is not sufficient to explain the increased proliferation of neuroepithelial cells. Instead, it appears more likely that interfering with dystroglycan function influences intracellular signaling processes involved in regulating the cell cycle. A key regulator for neuroepithelial cell proliferation is the intracellular phosphatase PTEN since loss of PTEN leads to increased proliferation of neuroepithelial cells resulting in an increase in brain size and altered CNS histoarchitecture (Groszer et al., 2001). Interestingly, recent studies have provided evidence that dystroglycan influences PTEN function (Muschler et al., 2002; Sgambato et al., 2006). Although further studies are needed, our results are consistent with the hypothesis that dystroglycan is a component of the signaling cascade regulating proliferation and differentiation of neuroepithelial stem cells. Moreover, since several studies have demonstrated a role of dystroglycan in the regulation of the cell cycle and cell division (see for example Sgambato et al., 2003; Brennan et al., 2004), the effect might not be restricted to neuroepithelial cells.

The dystroglycan protein is synthesized as a single polypeptide which is posttranslationally cleaved into the α- and β-subunit at a particular serine residue by an unknown protease (Ibraghimov-Beskrovnaya et al., 1992; Deyst et al., 1995). The significance of this cleavage is not known, but overexpression of a non-cleavable dystroglycan protein in skeletal muscle lead to muscular dystrophy in the transgenic mice, demonstrating that dystroglycan cleavage is essential for normal muscle function (Jayasinha et al., 2003). Heterologous expression of non-cleavable chick dystroglycan revealed that proteolytic cleavage was not necessary for synthesis, trafficking, normal glycosylation, and membrane localization of the mutated protein (Esapa et al., 2003). Likewise, overexpression of non-cleavable dystroglycan in neuroepithelial cells by *in ovo* electroporation did not apparently alter the expression of endogenous dystroglycan and the protein encoded by the non-cleavable construct had a molecular weight of approximately 160 kDa, consistent with normal glycosylation of the non-cleaved dystroglycan protein. However, expression of this construct in neuroepithelial cells resulted in less proliferation and less neuronal differentiation. Thus, our results for the first time provide evidence for a role of the proteolytic cleavage of dystroglycan in the developing CNS. In addition, neuroepithelial cells transfected with the non-cleavable dystroglycan construct showed a concentration of nuclei at the basal side raising the possibility that the interkinetic nuclear movement was terminated around S-phase of the cell cycle. Interestingly, recent studies have shown that heterologous expression of dystroglycan protein and mRNA in epithelial cells is cell cycle dependent and that suppression of dystroglycan synthesis with siRNA resulted in inhibition of cell growth, accumulation of cells in the S-phase of the cell cycle, and failure of differentiation (Sgambato et al., 2006), suggesting a specific influence of dystroglycan on proliferation that is not restricted to neuroepithelial cells.

In a previous study, mice with a human GFAP promoter-mediated brain-specific deletion of dystroglycan showed a fragmented pial basal lamina (Moore et al., 2002). Likewise, injection of morpholino antisense oligonucleotides into the four cell stage *Xenopus laevis* caused disruption of the basal lamina (Luniardi et al., 2006). In agreement with these results, we observed areas with a disorganized basal lamina in retinae transfected with RNAi targeting dystroglycan, suggesting that the continuous expression of dystroglycan is important for basal lamina assembly in the developing CNS. However, neither injection of Fab fragments nor overexpression of mutated dystroglycan constructs resulted in a fenestrated basal lamina, at least within the 3–5 days of analysis in our study, indicating that the hyperproliferation of neuroepithelial cells and the increased number of postmitotic neurons are most likely not the result of an impaired assembly of the extracellular matrix. Moreover, while the morpholino-mediated loss of dystroglycan caused an increased apoptosis, microphtalmia and formation of rosette-like structures within the retina (Luniardi et al., 2006), we did not observe signs of increased cell death and loss of dystroglycan function was associated with an increased rate of proliferation. However, in our study the antibodies or cDNAs

were applied directly to neuroepithelial cells and the short-term effects within 3 to 4 days were investigated. In contrast, Luniardi et al. (2006) applied the morpholino antisense already at the four cell stage, and therefore analyzed long term effects of dystroglycan loss of function already during gastrulation and neurulation.

The interaction of α-dystroglycan with several extracellular matrix proteins including laminin and agrin is mediated by the carbohydrate side chains and mutations in at least three glycosyltransferases cause an altered glycosylation and subsequently an impaired ability of dystroglycan to interact with extracellular matrix proteins (for review see Martin-Rendon and Blake, 2003; Muntoni et al., 2004). The mutations in the glycosyltransferases cause three forms of congenital muscular dystrophy: Walker–Warburg Syndrome, Muscle–Eye–Brain Disease and Fukuyama Congenital Muscular Dystrophy. These diseases are characterized by a progressive skeletal muscle degeneration and a particularly severe brain and retina phenotype, which includes hyperproliferation of neurons and glial cells, heterotopias, disorganized layering, defects in neuronal migration, fragmented basal laminae, and clusters of neurons and glial cells ectopially in the subarachinoidal space (for review see Muntoni et al., 2004). Likewise, mice with a CNS-specific deletion of dystroglycan in GFAP-expressing cells (Moore et al., 2002) or mice lacking one of the glycosyltransferases (Takeda et al., 2003; Michele et al., 2002; Kurahashi et al., 2005; Lee et al., 2005) develop a similar phenotype in the CNS. Our studies suggest for the first time that one of the main functions of dystroglycan and the DGC during early stages of CNS development is the anchoring of neuroepithelial cell endfeet to the basal lamina and suggest that at least some of the CNS abnormalities observed in these forms of congenital muscular dystrophy or in the corresponding mouse models might be explained by an altered function of dystroglycan or the DGC at the endfoot–basal lamina interface.

Acknowledgments

We would like to thank A. Maelicke and H. Wässle for support and encouragement, A. Rohrbacher, G. Krauβe and C. Ziegler for expert technical assistance, H. Rohrer and A. Wizenmann for help with the *in ovo* electroporation, D. Engelkamp for the help with the RNAi work, C. Krull for the gift of the pMES vector and F. Rathjen for providing the anti-Ng-CAM antibodies. The critical reading and improving of the manuscript by D. Schulte and S.C. Brown is gratefully acknowledged. This study was supported by the Deutsche Forschungsgemeinschaft (Kr 1039/7 to S.K.), the DFG Priority Program 1086 (Kr 1039/9 to S.K.), the NMFZ at the University of Mainz (J.E.S.) and the Forschungsfond of the University of Mainz (S.K.). D.J. Blake is a Wellcome Trust Senior Investigator.

Appendix A. Supplementary data

Supplementary data associated with this article can be found, in the online version, at doi:10.1016/j.ydbio.2007.04.020.

References

Anderson, J.L., Head, S.I., Rae, C., Morley, J.W., 2002. Brain function in Duchenne muscular dystrophy. Brain 125, 4–13.

Barresi, R., Campbell, K.P., 2006. Dystroglycan: from biosynthesis to pathogenesis of human disease. J. Cell Sci. 119, 199–207.

Belecky-Adams, T., Cook, B., Adler, R., 1996. Correlations between terminal mitosis and differentiated fate of retinal precursor cells in vivo and in vitro: analysis with the "window-labeling" technique. Dev. Biol. 178, 304–315.

Beltran-Valero, D.B., Currier, S., Steinbrecher, A., Celli, J., Van Beusekom, E., Van Der, Z.B., Kayserili, H., Merlini, L., Chitayat, D., Dobyns, W.B., Cormand, B., Lehesjoki, A.E., Cruces, J., Voit, T., Walsh, C.A., van Bokhoven, H., Brunner, H.G., 2002. Mutations in the *O*-mannosyltransferase gene POMT1 give rise to the severe neuronal migration disorder Walker–Warburg Syndrome. Am. J. Hum. Genet. 71, 1033–1043.

Beltran-Valero de Bernabe, D., Voit, T., Longman, C., Steinbrecher, A., Straub, V., Yuva, Y., Herrmann, R., Sperner, J., Korenke, C., Diesen, C., Dobyns, W.B., Brunner, H.G., van Bokhoven, H., Brockington, M., Muntoni, F., 2004. Mutations in the FKRP gene can cause muscle–eye–brain disease and Walker–Warburg Syndrome. J. Med. Genet. 41, e61.

Bewick, G.S., Nicholson, L.V.B., Young, C., O'Donnell, E., Slater, C.R., 1992. Different distributions of dystrophin and related proteins at nerve–muscle junctions. NeuroReport 3, 857–860.

Blake, D.J., Kröger, S., 2000. The neurobiology of Duchenne muscular dystrophy: learning lessons from muscle? Trends Neurosci. 23, 92–99.

Blake, D.J., Nawrotzki, R., Loh, N.Y., Gorecki, D.C., Davies, K.E., 1998. Beta-dystrobrevin, a member of the dystrophin-related protein family. Proc. Natl. Acad. Sci. U. S. A. 95, 241–246.

Blank, M., Koulen, P., Kröger, S., 1997. Subcellular concentration of β-dystroglycan in photoreceptors and glial cells of the chick retina. J. Comp. Neurol. 389, 668–678.

Blank, M., Blake, D.J., Kröger, S., 2002. Molecular diversity of the dystrophin-like protein complex in the developing and adult avian retina. Neuroscience 111, 259–273.

Bozzi, M., Veglia, G., Paci, M., Sciandra, F., Giardina, B., Brancaccio, A., 2001. A synthetic peptide corresponding to the 550–585 region of alpha-dystroglycan binds beta-dystroglycan as revealed by NMR spectroscopy. FEBS Lett. 499, 210–214.

Brennan, P.A., Jing, J., Ethunandan, M., Gorecki, D., 2004. Dystroglycan complex in cancer. Eur. J. Surg. Oncol. 30, 589–592.

Burkin, D.J., Wallace, G.Q., Nicol, K.J., Kaufman, D.J., Kaufman, S.J., 2001. Enhanced expression of the alpha 7 beta 1 integrin reduces muscular dystrophy and restores viability in dystrophic mice. J. Cell Biol. 152, 1207–1218.

Cerna, J., Cerecedo, D., Ortega, A., Garcia-Sierra, F., Centeno, F., Garrido, E., Mornet, D., Cisneros, B., 2006. Dystrophin Dp71f associates with the beta1-integrin adhesion complex to modulate PC12 cell adhesion. J. Mol. Biol. 362, 954–965.

Cohn, R.D., 2005. Dystroglycan: important player in skeletal muscle and beyond. Neuromuscul. Disord. 15, 207–217.

Cohn, R.D., Henry, M.D., Michele, D.E., Barresi, R., Saito, F., Moore, S.A., Flanagan, J.D., Skwarchuk, M.W., Robbins, M.E., Mendell, J.R., Williamson, R.A., Campbell, K.P., 2002. Disruption of Dag1 in differentiated skeletal muscle reveals a role for dystroglycan in muscle regeneration. Cell 110, 639–648.

Dalkilic, I., Kunkel, L.M., 2003. Muscular dystrophies: genes to pathogenesis. Curr. Opin. Genet. Dev. 13, 231–238.

Deng, W.M., Schneider, M., Frock, R., Castillejo-Lopez, C., Baumgartner, S., Ruohola-Baker, H., 2003. Dystroglycan is required for polarizing the epithelial cells and the oocyte in Drosophila. Development 130, 173–184.

Deyst, K.A., Bowe, M.A., Leszyk, J.D., Fallon, J.R., 1995. The alpha-dystroglycan–beta-dystroglycan complex. Membrane organization and relationship to an agrin receptor. J. Biol. Chem. 270, 25956–25959.

Durbeej, M., Larsson, E., Ibraghimov-Beskrovnaya, O., Roberds, S.L., Campbell, K.P., Ekblom, P., 1995. Non-muscle alpha-dystroglycan is involved in epithelial development. J. Cell Biol. 130, 79–91.

Durbeej, M., Talts, J.F., Henry, M.D., Yurchenco, P.D., Campbell, K.P., Ekblom, P., 2001. Dystroglycan binding to laminin alpha 1LG4 module influences

epithelial morphogenesis of salivary gland and lung in vitro. Differentiation 69, 121–134.
Ervasti, J.M., Campbell, K.P., 1993. A role for the dystrophin–glycoprotein complex as a transmembrane linker between laminin and actin. J. Cell Biol. 122, 809–823.
Esapa, C.T., Bentham, G.R.B., Schröder, J.E., Kröger, S., Blake, D.J., 2003. The effects of post-translational processing on dystroglycan synthesis and trafficking. FEBS Lett. 555, 209–216.
Götz, M., Huttner, W.B., 2005. The cell biology of neurogenesis. Nat. Rev., Mol. Cell Biol. 6, 777–788.
Graus-Porta, D., Blaess, S., Senften, M., Littlewood-Evans, A., Damsky, C., Huang, Z., Orban, P., Klein, R., Schittny, J.C., Müller, U., 2001. Beta 1-class integrins regulate the development of laminae and folia in the cerebral and cerebellar cortex. Neuron 31, 367–379.
Groszer, M., Erickson, R., Scripture-Adams, D.D., Lesche, R., Trumpp, A., Zack, J.A., Kornblum, H.I., Liu, X., Wu, H., 2001. Negative regulation of neural stem/progenitor cell proliferation by the Pten tumor suppressor gene in vivo. Science 294, 2186–2189.
Halfter, W., Schurer, B., 1998. Disruption of the pial basal lamina during early avian embryonic development inhibits histogenesis and axonal pathfinding in the optic tectum. J. Comp. Neurol. 397, 105–117.
Halfter, W., Reckhaus, W., Kröger, S., 1987. Nondirected axonal growth on basal lamina from avian embryonic neural retina. J. Neurosci. 7, 3712–3722.
Halfter, W., Dong, S.C., Yip, Y.P., Willem, M., Mayer, U., 2002. A critical function of the pial basement membrane in cortical histogenesis. J. Neurosci. 22, 6029–6040.
Hamburger, V., Hamilton, H.L., 1951. A series of normal stages in the development of the chick embryo. J. Morphol. 88, 48–92.
Haubensak, W., Attardo, A., Denk, W., Huttner, W.B., 2004. Neurons arise in the basal neuroepithelium of the early mammalian telencephalon: A major site of neurogenesis. Proc. Natl. Acad. Sci. U. S. A. 101, 3196–3201.
Haubst, N., Georges-Labouesse, E., De Arcangelis, A., Mayer, U., Götz, M., 2006. Basement membrane attachment is dispensable for radial glial cell fate and for proliferation, but affects positioning of neuronal subtypes. Development 133, 3245–3254.
Herrmann, R., Straub, V., Blank, M., Kutzick, C., Franke, N., Jacob, E.N., Lenard, H.G., Kröger, S., Voit, T., 2000. Dissociation of the dystroglycan complex in caveolin-3-deficient limb girdle muscular dystrophy. Hum. Mol. Genet. 9, 2335–2340.
Huang, X., Poy, F., Zhang, R.G., Joachimiak, A., Sudol, M., Eck, M.J., 2000. Structure of a WW domain containing fragment of dystrophin in complex with beta-dystroglycan. Nat. Struct. Biol. 7, 634–638.
Ibraghimov-Beskrovnaya, O., Ervasti, J.M., Leveille, C.J., Slaughter, C.A., Sernett, S.W., Campbell, K.P., 1992. Primary structure of dystrophin-associated glycoproteins linking dystrophin to the extracellular matrix. Nature 355, 696–702.
Jayasinha, V., Nguyen, H.H., Xia, B., Kammesheidt, A., Hoyte, K., Martin, P.T., 2003. Inhibition of dystroglycan cleavage causes muscular dystrophy in transgenic mice. Neuromuscul. Disord. 13, 365–375.
Judge, L.M., Haraguchiln, M., Chamberlain, J.S., 2006. Dissecting the signaling and mechanical functions of the dystrophin–glycoprotein complex. J. Cell Sci. 119, 1537–1546.
Jung, D., Yang, B., Meyer, J., Chamberlain, J.S., Campbell, K.P., 1995. Identification and characterization of the dystrophin anchoring site on β-dystroglycan. J. Biol. Chem. 270, 27305–27310.
Kriegstein, A.R., Götz, M., 2003. Radial glia diversity: a matter of cell fate. Glia 43, 37–43.
Kriegstein, A.R., Noctor, S.C., 2004. Patterns of neuronal migration in the embryonic cortex. Trends Neurosci. 27, 392–399.
Kröger, S., 1997. Differential distribution of agrin isoforms in the developing and adult avian retina. Mol. Cell. Neurosci. 10, 149–161.
Kröger, S., Schwarz, U., 1990. The avian tectobulbar tract: development, explant culture, and effects of antibodies on the pattern of neurite outgrowth. J. Neurosci. 10, 3118–3134.
Kröger, S., Horton, S.E., Honig, L.S., 1996. The developing avian retina expresses agrin isoforms during synaptogenesis. J. Neurobiol. 29, 165–182.
Kumar, R., Conklin, D.S., Mittal, V., 2003. High-throughput selection of effective RNAi probes for gene silencing. Genome Res. 13, 2333–2340.
Kurahashi, H., Taniguchi, M., Meno, C., Taniguchi, Y., Takeda, S., Horie, M., Otani, H., Toda, T., 2005. Basement membrane fragility underlies embryonic lethality in fukutin-null mice. Neurobiol. Dis. 19, 208–217.
Layer, P.G., Sporns, O., 1987. Spatiotemporal relationship of embryonic cholinesterases with cell proliferation in chicken brain and eye. Proc. Natl. Acad. Sci. USA 84, 284–288.
Lee, Y., Kameya, S., Cox, G.A., Hsu, J., Hicks, W., Maddatu, T.P., Smith, R.S., Naggert, J.K., Peachey, N.S., Nishina, P.M., 2005. Ocular abnormalities in Largemyd and Largevls mice, spontaneous models for muscle, eye, and brain diseases. Mol. Cell. Neurosci. 30, 160–172.
Lemmon, V., Rieser, G., 1983. The developmental distribution of vimentin in the chick retina. Dev. Brain Res. 11, 191–197.
Longman, C., Brockington, M., Torelli, S., Jimenez-Mallebrera, C., Kennedy, C., Khalil, N., Feng, L., Saran, R.K., Voit, T., Merlini, L., Sewry, C.A., Brown, S.C., Muntoni, F., 2003. Mutations in the human LARGE gene cause MDC1D, a novel form of congenital muscular dystrophy with severe mental retardation and abnormal glycosylation of alpha-dystroglycan. Hum. Mol. Genet. 12, 2853–2861.
Luniardi, A., Cremisi, F., Dente, L., 2006. Dystroglycan is required for proper retinal layering. Dev. Biol. 290, 411–420.
Martin-Rendon, E., Blake, D.J., 2003. Protein glycosylation in disease: new insights into the congenital muscular dystrophies. Trends Pharmacol. Sci. 24, 178–183.
Michele, D.E., Barresi, R., Kanagawa, M., Saito, F., Cohn, R.D., Satz, J.S., Dollar, J., Nishino, I., Kelley, R.I., Somer, H., Straub, V., Mathews, K.D., Moore, S.A., Campbell, K.P., 2002. Post-translational disruption of dystroglycan–ligand interactions in congenital muscular dystrophies. Nature 418, 417–422.
Momose, T., Tonegawa, A., Takeuchi, J., Ogawa, H., Umesono, K., Yasuda, K., 1999. Efficient targeting of gene expression in chick embryos by microelectroporation. Dev. Growth Differ. 41, 335–344.
Moore, S.A., Saito, F., Chen, J.G., Michele, D.E., Henry, M.D., Messing, A., Cohn, R.D., Ross-Barta, S.E., Westra, S., Williamson, R.A., Hoshi, T., Campbell, K.P., 2002. Deletion of brain dystroglycan recapitulates aspects of congenital muscular dystrophy. Nature 418, 422–425.
Muntoni, F., Brockington, M., Torelli, S., Brown, S.C., 2004. Defective glycosylation in congenital muscular dystrophies. Curr. Opin. Neurol. 17, 205–209.
Muschler, J., Levy, D., Boudreau, R., Henry, M., Campbell, K., Bissell, M.J., 2002. A role for dystroglycan in epithelial polarization: loss of function in breast tumor cells. Cancer Res. 62, 7102–7109.
Neumann, F.R., Bittcher, G., Annies, M., Schumacher, B., Kröger, S., Ruegg, M.A., 2001. An alternative amino-terminus expressed in the central nervous system converts agrin to a type II transmembrane protein. Mol. Cell. Neurosci. 17, 208–225.
Randall, W.R., Tsim, K.W.K., Lai, J., Barnard, E.A., 1987. Monoclonal antibodies against chicken brain acetylcholinesterase: their use in immuno-purification and immunochemistry to demonstrate allelic variants of the enzyme. Eur. J. Biochem. 164, 95–102.
Rando, T.A., 2001. The dystrophin–glycoprotein complex, cellular signaling, and the regulation of cell survival in the muscular dystrophies. Muscle Nerve 24, 1575–1594.
Rathjen, F.G., Wolff, J.M., Frank, R., Bonhoeffer, F., Rutishauser, U., 1987. Membrane glycoproteins involved in neurite fasciculation. J. Cell Biol. 104, 343–353.
Rybakova, I.N., Amann, K.J., Ervasti, J.M., 1996. A new model for the interaction of dystrophin with F-actin. J. Cell Biol. 135, 661–672.
Saito, Y., Murayama, S., Kawai, M., Nakano, I., 1999. Breached cerebral glia limitans–basal lamina complex in Fukuyama-type congenital muscular dystrophy. Acta Neuropathol. 98, 330–336.
Sauer, F.C., 1935. Mitosis in the neural tube. J. Comp. Neurol. 62, 377–405.
Sciandra, F., Schneider, M., Giardina, B., Baumgartner, S., Petrucci, T.C., Brancaccio, A., 2001. Identification of the beta-dystroglycan binding epitope within the C-terminal region of alpha-dystroglycan. Eur. J. Biochem. 268, 4590–4597.
Sgambato, A., Migaldi, M., Montanari, M., Camerini, A., Brancaccio, A., Rossi, G., Cangiano, R., Losasso, C., Capelli, G., Trentini, G.P., Cittadini, A., 2003. Dystroglycan expression is frequently reduced in human breast and colon cancers and is associated with tumor progression. Am. J. Pathol. 162, 849–860.

Sgambato, A., Di Salvatore, M.A., De, P.B., Rettino, A., Faraglia, B., Boninsegna, A., Graziani, C., Camerini, A., Proietti, G., Cittadini, A., 2006. Analysis of dystroglycan regulation and functions in mouse mammary epithelial cells and implications for mammary tumorigenesis. J. Cell. Physiol. 207, 520–529.

Shcherbata, H.R., Yatsenko, A.S., Patterson, L., Sood, V.D., Nudel, U., Yaffe, D., Baker, D., Ruohola-Baker, H., 2007. Dissecting muscle and neuronal disorders in a *Drosophila* model of muscular dystrophy. EMBO J. 26, 481–493.

Spence, H.J., Dhillon, A.S., James, M., Winder, S.J., 2004. Dystroglycan, a scaffold for the ERK-MAP kinase cascade. EMBO Rep. 5, 484–489.

Sugita, S., Saito, F., Tang, J., Satz, J., Campbell, K., Südhof, T.C., 2001. A stoichiometric complex of neurexins and dystroglycan in brain. J. Cell Biol. 154, 435–445.

Sugiyama, J., Bowen, D.C., Hall, Z.W., 1994. Dystroglycan binds nerve and muscle agrin. Neuron 13, 103–115.

Swartz, M., Eberhart, J., Mastick, G.S., Krull, C.E., 2001. Sparking new frontiers: using in vivo electroporation for genetic manipulations. Dev. Biol. 233, 13–21.

Takeda, S., Kondo, M., Sasaki, J., Kurahashi, H., Kano, H., Arai, K., Misaki, K., Fukui, T., Kobayashi, K., Tachikawa, M., Imamura, M., Nakamura, Y., Shimizu, T., Murakami, T., Sunada, Y., Fujikado, T., Matsumura, K., Terashima, T., Toda, T., 2003. Fukutin is required for maintenance of muscle integrity, cortical histogenesis and normal eye development. Hum. Mol. Genet. 12, 1449–1459.

Talts, J.F., Andac, Z., Gohring, W., Brancaccio, A., Timpl, R., 1999. Binding of the G domains of laminin alpha 1 and alpha 2 chains and perlecan to heparin, sulfatides, alpha-dystroglycan and several extracellular matrix proteins. EMBO J. 18, 863–870.

Yoshida, A., Kobayashi, K., Manya, H., Taniguchi, K., Kano, H., Mizuno, M., Inazu, T., Mitsuhashi, H., Takahashi, S., Takeuchi, M., Herrmann, R., Straub, V., Talim, B., Voit, T., Tapaloglu, H., Toda, T., Endo, T., 2001. Muscular dystrophy and neuronal migration disorder caused by mutations in a glycosyltransferase, POMGnT1. Dev. Cell 1, 717–724.

Zaccaria, M.L., Di Tommaso, F., Brancaccio, A., Paggi, P., Petrucci, T.C., 2001. Dystroglycan distribution in adult mouse brain: a light and electron microscopy study. Neuroscience 104, 311–324.